PREDICTING THE EFFECTS OF GREEN ROOFED URBAN BUILDINGS ON COOLING LOADS

SADIQ ABUBAKAR GULMA

MASTER OF SCIENCE

ENVIRONMENTAL AND ASAL ENGINEERING

PAN AFRICAN UNIVERSITY

INSTITUTE FOR BASIC SCIENCES, TECHNOLOGY AND INNOVATION

2014

PREDICTING THE EFFECTS OF GREEN ROOFED URBAN BUILDINGS ON COOLING LOADS

SADIQ ABUBAKAR GULMA

CE300-0001/12

A THESIS SUBMITTED TO PAN AFRICAN UNIVERSITY, INSTITUTE FOR BASIC SCIENCES, TECHNOLOGY AND INNOVATION IN PARTIAL FULFILMENT OF THE REQUIREMENTS FOR THE DEGREE OF

MASTER OF SCIENCE

(CIVIL ENGINEERING - ENVIRONMENTAL AND ARID AND SEMI-ARID LANDS OPTION)

2014

DECLARATION

This thesis is my original work and has not been submitted to any other university for examination.

Signature: _____ Date: _____

Sadiq Abubakar Gulma

This thesis report has been submitted for examination with our approval as University supervisors.

Signature: _____ Date: _____

Dr Patrick Ajwang

JKUAT, Kenya

Signature: _____ Date: _____

Dr Stephen N. Ondimu

JKUAT, Kenya

DEDICATION

I heartily dedicate this work to all those who fight for the protection of our environment.

ACKNOWLEDGEMENT

My deepest gratitude goes to God for sparing my life until this moment and granting me the ability to carry out this thesis. I wish to extend my gratefulness to the African Union Commission, who awarded me a generous scholarship for two years to undertake my masters' degree. To thank the most important people associated with this thesis, without which I do not know the dimension it will take, my supervisors, Dr Patrick Ajwang and Dr Stephen Ondimu who always devote their precious time in attending to me, I feel indebted to all of you forever. Thank you very much for your guidance and relentless effort towards my success. Other academic and non-academic staff of Biomechanical and Environmental Engineering Department, especially the chair, Dr U. Mutwiwa, who has been present since the inception of this research, and has provided meaningful critiques to the study, thank you. Professor Patrick Home, who instilled in me, research skills and interests early before my thesis started, the whole academic stay in Kenya would have been something less than average. I also wish to heartily acknowledge your constant mentoring, guidance and being a friend also. Mr Robert Ogeto and Mr Teresphorus Mutunga, I am grateful for the immense help you offered for my experimental study, which happens to be the cardinal point of this thesis. I am equally grateful to all the staff of PAUISTI, JKUAT and AICAD who facilitated our study. Cheerful colleagues and friends from PAU, JKUAT, USIU, AIESEC and IAESTE, who I cannot have imagined how life would be without you guys, thanks for all the moral support you offered. My parents back home, who have given me the best thing ever, education and moral character, I am eternally grateful and ask only God to repay you, as it is out of my reach to do that

myself. My siblings, relatives, Ahmed Jari, Sabo Aliyu, Mallan Lawan Adamu, friends, and everyone I might have skipped in this acknowledgement because of space, you have all contributed to this accomplishment, a hearty thanks and hugs to all of you.

TABLE OF CONTENTS

LIST OF TABLES

LIST OF FIGURES

LIST OF PLATES

LIST OF DEFINITION OF TERMS

Microclimate: It is the climate of a small area that is different from the area around it. It may be warmer or colder, wetter or drier, or more or less prone to frosts.

Physical model: A model structure can be built on physical grounds, which has a certain number of parameters to be estimated from data.

White-box model: This is the case when a model is perfectly known; it has been possible to construct it entirely from prior knowledge and physical insight.

Grey-box model: This is the case when some physical insight is available, but several parameters remain to be determined from observed data

Black-box model: No physical insight is available or used, but the chosen model structure belongs to families that are known to have good flexibility and have been "successful in the past".

Green roof: It is basically any roof that a green technology has been incorporated on it.

Bioclimatic design: the design of buildings and spaces based on local climate.

Energy efficient building: building as a structure, owning to its site location and construction material, consumes less energy for heating or cooling purposes, while minimizing the need for anthropogenic heating or cooling.

LIST OF NOMENCLATURE

Q_r	radiant energy [w]
A	area of the building surface [m^2]
ε	emissivity of the building [-]
Ts	temperature of the building exposed surface [K],
Tsky	sky temperature [K]
R	overall thermal resistance per unit area
U	overall thermal transmittance [$W/m^2/K$]
Q	Heat flow [w]
T_i,t_i	indoor temperature,
T_o, t_o	outdoor temperature
f_i and f_o	inside and outside heat transfer coefficients
L_j	thickness of the *jth* layer
K_j	thermal conductivity of *jth* material
C:	The thermal conductance
$Qr_{(in)}$	solar radiant energy into the building [w/m^2]
$Qr_{(out)}$	solar radiant energy outside the building [w/m^2]
Tr:	Transmissivity of the wall material [-]
Q_{cd}	Quantity of heat flow/ Heat flux due to conduction [w]
k	thermal conductivity of the material [w/m/k]
ΔT	Temperature difference of the two media [K]
D	Thickness of the material [m]
Q_T	Total energy that comes into the house [w]
Q_W	Energy loss through the walls [w]
Q_F	Energy loss into the floor [w]
Q_G	Energy loss through the glazing (window) [w]
Q_R	Energy loss through the green roof [w]
Q_D	Energy loss through the door [w]

Greek letters

σ	Stefan-Boltzmann constant [$5.67 * 10^{-8}\ W/m^2K^4$]

Subscripts

Cd	Conduction
In	Inside
Out	Outside
i	Indoor
o	Outdoor
T	Total energy into the house
W	Wall
F	Fenestration
G	Glazing
R	Roof
D	Door
s	sky

dT/dx	temperature gradient in x-direction (k/m)

LIST OF ABBREVIATIONS AND ACRONYMS

AC: Air conditioning

ASHRAE: American Society of Heating, Refrigerating and Air conditioning Engineers

BMS: Building Management Systems

BRUB: Bare Roofed Urban Building

CPE: Chlorinated Polyethylene

CPSE: Chlorosulfonated Polyethylene

GRUB: Green Roofed Urban Building

EPDM: Ethylene-Propylenediene-Tetrolymer Membrane

HVAC: Heating, Ventilating and Air Conditioning

UCL: Urban Canopy Layer

UHI: Urban Heat Island

PVC: Polyvinyl Chloride

TPO: Thermoplastic Polyolefin

ABSTRACT

There is a growing use of living green roofs in some parts of the world to reduce heat gain into houses. The reduction of heat gain or loss into buildings automatically reduces energy consumption or combats urban heat island effect in cities, which also reduces energy consumption of buildings on a wide scale. This study was necessitated by the need to determine the potential reduction of cooling loads that can be realized by using living green roofs on building roof tops located in urban areas. The objectives set out to be achieved were to develop a computer model for predicting indoor air temperature in living green roofs, assess the potential reduction of energy consumption from using living greens and evaluate the differences between the indoor microclimate of a green roofed urban building and a bare roofed urban building. Two field scale urban like houses were constructed in Jomo Kenyatta University of Agriculture and Technology campus, Juja, Nairobi. One room had a living green roof and the other room's roof was left bare. There was no any form of ventilation for the two models, both natural and mechanical. Sensors were placed within and outside the physical models to monitor microclimate parameters. The green roof was interchanged for the two houses and field observation continued. The total period of obtaining the data was from 28th April to 6th July, 2014. A new thermodynamic model called GRUBCLIM was developed to predict the indoor temperature of green roofed urban buildings. Modelling and simulation were carried out in SIMULINK. The model was validated with data measured at the field scale model site and simulated with another set of different of data. A correlation of 0.885 was met between predicted and obtained values. The energy savings potential of the green roofs were

determined based on the heat gain/loss in the green roofed urban building and the bare roof urban building. Results show that during the daytime, a mean heat gain reduction of approximately 63% was recorded for the house with the living green roof when compared with the bare roofed house. The indoor microclimates of both rooms, green roofed and bare roof urban buildings were investigated to determine the differences in temperature and relative humidity. A mean daytime value of 22.86 °C was recorded for the green roofed building while that with a bare roof recorded a higher value of 24.48 °C.

CHAPTER ONE

INTRODUCTION

1.1 Background to the Problem

It is known that urban climates differ from those of rural areas and that the magnitudes of the differences can be quite large at times depending on weather conditions, urban thermophysical and geometrical characteristics, and anthropogenic moisture and heat sources present in the area (Taha, 1997). The large areas modern cities occupy, their structure, materials and the general lack of vegetation have altered the climatic characteristics of urban spaces (Alexandri and Jones, 2006). The fluxes of heat, moisture, and momentum are significantly altered by the urban landscape and the contrast between the urban and 'undisturbed' climates is further enhanced by the input of anthropogenic heat, moisture, and pollutants into the atmosphere (Taha, 1997). Landsberg, 1981 (as cited in Priyadarsini, 2008) mentioned that the concrete used in buildings, the asphalting of the roadways, the different roofing materials and so many types of materials used in urban surfacing are the basis for the heat absorption and as a consequence of changes in the heat balance, air temperatures in densely built urban areas are higher than the temperatures of the surrounding area.

This phenomenon, known as Urban Heat Island (UHI), Landsberg (1981) mentioned, has been recognized since the turn of this century. It is a reflection of the totality of microclimatic changes brought about by man-made alterations of the urban surface. A

heat island can occur at a range of scales; it can manifest itself around a single building (Thurow, 1983), a small vegetative canopy (Taha et al., 1989, Taha et al, 1991), or a large portion of a city. According to Taha (1997), depending on geographic location and prevailing weather conditions, heat islands may be beneficial or detrimental to the urban dweller and energy user. As cited in Madhumathi and Sundarraja (2012), Humphreys and Nicol (2000) discovered that the indoor thermal comfort temperatures are linearly related to the mean outdoor temperature; hence, justifying the claim that outside microclimate plays a very influential role in the indoor temperature, or rather the thermal comfort, perception for a free standing building.

Hassid et al., 2000 in a study (as cited in Santamouris, 2012) showed higher urban temperatures increase the energy consumption for cooling of indoor spaces and raise the peak electricity demand. Energy usage in buildings for heating and cooling in the US have costed about US $40 billion (Akbari, 2002). Akbari (2002) noted that urban trees can improve urban thermal comfort in hot climates. He found out that about $270 million worth of energy could be saved in the city of Los Angeles if urban trees had existed for about 15-20 years. Air conditioning, the artificial and mechanical way of cooling buildings is the most widely used system, albeit they have a great energy expenditure (Barrio, 1998). About a third of energy consumption in the world is attributed to buildings. In developed countries, it accounts for around half of primary energy usage (Castleton et al., 2010), 39% of Great Britain, 25% of Japan, 42% of Brazil, 47% of Switzerland and 28% of China (Saadatian, 2013). A great proportion of this energy is used in heating and cooling systems.

In cases where little cooling load is needed, cooling demand can be reduced to zero by covering building surfaces with vegetation (Sadaatian et al., 2013). In other cases, energy savings can also be significant, varying from 90% to 35% (Sadaatian et al., 2013). In addition to the energy savings themselves, this could lead to successful applications of further passive cooling techniques, especially those employing ventilation, which are not easy to implement in the extremely hot urban conditions, in cases of large heat island densities (Alexandri and Jones, 2006).

Barrio (1998) mentioned that in early times, natural cooling techniques have been used to cool off buildings, however, its use faded away in recent decades. The use of green roofs dates back to centuries ago (Sailor, 2008). However, they were not used to modify or insulate buildings then, but as a protective cover to prolong the life cycle of roofs. A green roof constitutes a layered structure of waterproofing membrane, growing medium and the vegetation layer itself (Castleton et al., 2010, Ondimu & Murase, 2007, Sailor, 2008). More generally, it refers to any type of roof that a green technology has been incorporated (Saadatian et al., 2013). Because of their ability to reduce the proportion of solar radiation that reaches the roof beneath (Castelton et al, 2010) and subsequent penetration into the building, it possess the potential in reducing the energy (Chen, 2013) that will have been used in cooling the higher heated spaces.

The process by which green roofs cool has been decribed by Castleton et al. (2010) and Chen (2013); they explained that green roofs cool by latent heat loss and improved reflectivity of incident solar radiation. The numerous benefits of green roofs, both to the

building and the environment have been mentioned by so many authors (Chen, 2013; Castleton et al., 2010). Experimentation of other researchers showed that a possible reduction of cooling load between 6% and 49% could be achieved. Castleton et al. (2010) noted that planted roots suffer less heat gain during the day. Chen (2013) stated that vegetated roofs dissipate more heat than bare roofs. Furthermore, Chen stated that with green roofs, both inside and outside temperature fluctuate less hence, enabling them to save more on energy and reduce carbon emissions.

Since antiquity, human beings have clearly intended to alter their microclimate to a more ‘‘human friendly’’ one, protecting themselves from extreme climatic conditions (Alexandri and Jones, 2006). In justifying why comforting conditioning is needed by human beings, Jones (1985) stated that human beings are born into a hostile environment, and the degree of hostility varies with the geography and seasons of the locality. According to ASHRAE Comfort standard 55-74, comfort is defined as ‘...that state of mind which expresses satisfaction with the thermal environment...’ however, other researchers mentioned that the definition of comfort is a subjective sensation that is expressed by an individual, when questioned, as neither slightly warm nor slightly cool.

Briefly, the need for air conditioning arises due to heat gains from sunlight and electric lighting-which causes high temperature in rooms-unless windows are opened to let in the natural air ventilate the place. When the windows are open, other unwanted comfort levels might be reached such as draughts caused by wind, noise, dirt and odorous smell can flow in.

Jones (1985) published a book about air conditioning engineering and defined full air conditioning as the automatic control of an atmospheric environment either for the comfort of human beings or animals or for the proper performance of some industrial or scientific process. However, fulfilling this intention of satisfactory environment condition is a task which has faced mankind throughout history (Martin & Oughton, 1995). Before the advent of air conditioners and mechanical ventilation systems, various forms of protection against the elements of weather have been provided by structures suited to individual circumstances, the techniques being related to the severity of the local climatic conditions, to the materials which were available and to the skills of the builders (Martin & Oughton, 1995).

According to Madhumathi and Sundarraja (2012), a building's mass plays an important role in determining the inner temperature of the building. They reported on the use of thermal mass in shelter as a strategy for building climate control in hot regions. However, current practices in construction of buildings have seen a paradigm shift in the use of construction materials used. Lightweight construction materials have an effect on the inner microclimate and are constantly being preferred over conventional heavy materials. The slim thickness of the materials raises concern over the internal comfort conditions due to lack of thermal storage properties resulting in rapid swings of indoor temperature (Madhumathi and Sundarraja, 2012). Optimized selection of building materials for making the external envelop plays an important role in achieving thermal comfort in buildings, where thermal comfort is achieved through passive – cooling, strategies.

The need to design buildings in consideration of the climate is imperative contemporarily as previous researches have shown the existence of potential benefits. Such potential benefits translate to designing buildings that consume less energy for heating or cooling purposes, otherwise known as energy efficient buildings. Mills (1997) defined energy efficient buildings as a structure, owning to its site location and construction material, accomplishes this task while minimizing the need for anthropogenic heating or cooling. Hui (2007) referred to the design of buildings and spaces based on local climate as "bioclimatic design". A bioclimatic design aims at providing thermal and visual comfort by making use of solar energy and other environmental sources in the natural energy flow. Mills (1997) mentioned that urban climatology research is completed with a goal of providing an understanding of the relationship between buildings and climate which may be employed in the field of urban design or urban planning.

1.2 Statement of the Problem

Energy used for room heating, cooling and ventilation accounts for more than one-third of the total primary energy demand in the industrialized countries, and is in this way a major polluter of the environment (Hakansson et al., 2012). About 40 million metric tons of carbon emission is attributed to energy used in air conditioning buildings in cities classified as heat-islands (Akbari, 2002). As mentioned by Santamouris et al. (2001), heat island in the city of Athens, Greece, doubles the cooling load of buildings and almost triples their peak electricity demand, while decreasing the Coefficient of Performance of mechanical cooling systems up to 25%. In the United States, 1° C increase in temperature

would increase peak electricity demand by 2-4% when temperature exceeded 15-20° C (Akbari et al., 1992). A temperature difference of up to 10 K between the denser urban and surrounding rural area can be reached (Akbari et al., 1992). The difference is about 7 K between London and its surrounding areas at night time (Watkins et al., 2013). UHI of the Urban Canopy Layer (UCL), can increase energy consumption, increase ambient air temperature, and reduce human thermal comfort (Oke, 1976).

Indoor microclimate of urban buildings is constantly deteriorating due to increased outdoor urban microclimate. Higher urban temperatures are due to the positive thermal balance of urban areas caused by the important release of anthropogenic heat, the excess storage of solar radiation by the city structures, the lack of green spaces and cool sinks, the non-circulation of air in urban canyons and the reduced ability of the emitted infrared radiation to escape in the atmosphere (Oke et al., 1991). Each of these causes modifies urban microclimate in different ways. These modifications have negative impacts on the well-being of people, both the local and global climate, and the energy consumption of buildings.

1.3 Justification

Since urbanization will continue to occur and cannot be stopped (by 2050, more than 70% of the world's population is expected to live in urban areas [UN, 2011]); it is certain that the local climate of urban regions will continue to change due to the developments. This change will affect wind flow and land use changes, of which, both will increase the heat flux of the region (Oliveira et al., 2011). These changes in heat flux outside the buildings

will affect the inner microclimate of the buildings by increasing the temperature uncomfortably. These temperatures also mean there would be more energy consumption for cooling the buildings. Other researches carried out for predicting the inner microclimate of buildings mostly considered the effect of different thermal masses (Ogoli, 2003; Givoni, 1998). In Egypt, Fathy (1986) reported on his findings about prediction of microclimate based on different construction materials.

Consequently, this study shifts the main focus to the outdoor microclimate and the incorporation of vegetation on the roof of the physical model. In all the studies of green roofs in the world (Singapore, Athens, Taiwan, South Korea, Japan, China, Hong Kong, [Chen, 2013]), there has been no documented research of green roofs carried out in Kenya thus necessitating this research appropriate for the local climate.

Furthermore, it is important to note that an individual house owner may have little or no control of the design of his neighbourhood and the developments in it, or the control of sunshine, or the cost of electricity in the city. However, the individual has control over how energy is consumed or what fraction of sunshine goes into his/her house; therefore, he/she can design or employ certain features on the building envelope to make it energy efficient (bioclimatic design).

The no-ventilation condition maintained as part of the experiment portrays the scenario where indoor spaces of buildings are kept closed whilst air conditioning (AC) systems are operating. Both windows and doors are kept shut while ACs are operating so as to maintain indoor temperatures and prevent their fluctuations. Furthermore, the windows

are at times shut in order to represent a scenario where unwanted conditions such as air pollution and noise pollution are prevented from getting into the building.

Positive results from this study can witness a paradigm shift in the way roofs and buildings are designed and constructed. The positive result could be reduction of energy consumption of heating and cooling devices, reduction in indoor temperatures and also stable maintenance of indoor temperature. With massive global calls for reductions of carbon emissions, policy makers and city planners could benefit from the outcomes of this study because less consumption of energy, which mainly comes from fossil fuel, would means less emission of carbon into the atmosphere.

1.4 Research Questions

1. What parameters are pertinent for developing a microclimate model for predicting the indoor microclimate of green roofed urban building?
2. What is the effect of a living green roof on energy cooling loads of urban buildings at no-ventilation?
3. What is/are the difference(s) between the indoor thermal environment of green roof urban buildings and bare roof urban buildings at no-ventilation?

1.5 Objectives

1.5.1 General Objective

To determine the effect of roof greening on energy consumption of urban buildings at no-ventilation.

1.5.2 Specific Objectives

1. To develop a computer model for predicting indoor microclimate of green roofed urban buildings.
2. To evaluate the effect of green roofing on energy cooling loads of urban buildings at no-ventilation.
3. To compare the indoor microclimates of green roofed urban buildings and bare roofed urban buildings.

1.6 Research Gaps

From the above review, it is certain that many researchers have looked at the possible reduction of cooling loads resulting from using green roofs in some cities. Others developed models for predicting cooling energy reductions and indoor microclimate of buildings from different aspects; thermal properties of building (envelope) materials, using outdoor temperatures and climate or region specific. While some studies of green roof have been made in some continents, many African cities are yet to be studied. Similarly, most researches have incorporated the effect of natural ventilation in their thermodynamic prediction models.

Hence, this research of studying the effects of a living green roof addresses regional, climatic and indoor objectives by conducting the field experiments in Kenya, Africa. The field experiments was done in a manner similar to the way urban buildings are cooled when air conditioning systems are operating; with all windows closed (no ventilation).

CHAPTER TWO

LITERATURE REVIEW

2.1 Introduction

The literature review of this thesis is discussed in three main topics; microclimate and thermal models used for prediction; energy usage of buildings and use of vegetation on buildings. The microclimate models reviewed are those developed by other researchers to predict indoor temperatures for different settings of houses. The secondly reviews the way and manner buildings receive heat and consume energy (referring to heating and cooling equipment that expend power). Lastly, documentation of where, how and for what vegetation has been used on buildings was covered.

2.2 Microclimate Models

2.2.1 Microclimate Prediction

A number of studies have been done for understanding and predicting indoor microclimate parameters with a focus on how building facades such as walls and roofs affect it (Ogoli, 2003), (Givoni, 2003), (Madhumathi and Sundarraja, 2012), (Cheng, Ng and Givoni, 2005). There are different ways in which modelling of microclimate can be done including but not limited to mechanistic, system identification, artificial neural networks etc. (Ajwang, 2005). Mechanistic modelling makes use of certain fundamental laws to build a description of process. These are the balance equations that describe the conservation of mass and the conservation of energy. Mechanistic modelling is very

expensive in terms of human effort and expertise. It requires large amount of representative data and in many cases can only be acquired by perturbing the process via planned experiments (Tham, 2000). Mechanistic models are used to provide more realistic predictions and more can be done in terms of analysis. It offers opportunities to test the sensitivities of the process to meaningful entities such as heat transfer coefficients (Tham, 2000).

The paper by Ljung (2011) elaborated greatly on system identification as follows. System identification models can be both; without any use of physical laws or with a little understanding of them. The models are termed *white-box, grey-box* or *black-box* models depending on the knowledge of physical laws employed. The *White Box* model which represents the case when it is possible to construct a model from prior knowledge and physical insight, in other words, the system behaviour is perfectly known. The *Grey Box* model represents a case when some physical insight is available but several parameters remain to be determined from observed data. And finally, the *Black box* model in which no physical knowledge is available or used but the chosen model structure belongs to families that are known to have good flexibility and have been "successful in the past" (Ljung, 2011).

According to Salat (2013), mathematical models resulting from system identification are used for the purpose of controlling, simulation tests and forecasting. However, it is difficult to find a mathematical model which is capable of accurately mapping a dynamic behaviour of the system (Salat, 2013). Sjoberg et al., (1995) pointed out that a key

problem in system identification is to find a suitable model structure, within which a good model is to be found. They distinguished customary ways (*white, grey or black*) in which one should utilize prior knowledge and physical insight about the system when selecting the model structure.

2.2.2 Review of Models

Ogoli (2003) carried out a research in the city of Nairobi for predicting indoor temperatures in closed buildings with high and low thermal masses. His focus was mainly on the effect of thermal mass on indoor comfort conditions, using the predicted indoor temperatures as an indicator of the thermal comfort. He built test chambers in a site with vegetation and considered different ceiling configurations. Two test chambers had timber walls while the other two chambers had natural stone work. His final model is presented in equation (2.1):

$$T_{\max-in} = T_{\max-out} - 0.488(T_{\max-out} - T_{\min-out}) + 2.44 \qquad (2.1)$$

Where

$T_{\text{max-in}}$ is the indoor maximum temperature;

$T_{\text{max-out}}$ the outdoor maximum temperature; and

$T_{\text{min-out}}$ is the outdoor minimum temperature.

In predicting the expected indoor maximum air temperature for high mass buildings, a statistical correlation between the predicted and the measured values arrived at a correlation of 0.83 while that of low mass buildings was 0.82, signifying a good model.

As cited in Ogoli (2003), Drysdale conducted a research in Australia (30°S) and suggested the following formula for predicting indoor maximum temperature for single-story buildings:

$$T_{\max-in} = T_{\max-out} - 0.009W(T_{\max-out} - 68) \quad (2.2)$$

Where $T_{\text{max-in}}$ is the indoor maximum temperature; $T_{\text{max-out}}$ the outdoor maximum temperature; and W is the average weight per unit area of the external walls (lb/ft2).

In India (20°N), Raychaudhury and Chaudhury (1961) suggested the following:

$$T_{\max-in} = T_{\max-out} - 0.004W \times (T_{\max-out} - 60) \quad (2.3)$$

Where

$T_{\text{max-in}}$ is the indoor maximum temperature;

$T_{\text{max-out}}$ the outdoor maximum temperature; and

W is the average weight of the whole structure, including roof, and the external walls, per unit area of the whole external surface (kg/m^2).

Ajwang's (2005) work for prediction of the effects of insect-proof screens on the climate in naturally ventilated greenhouses in the humid tropics, developed a thermodynamic model for predicting the indoor temperature of the greenhouse. The thermodynamic model is shown below:

$$(R_n - 0.08R_n)A - \rho_a C_p \phi_a (T_i - T_o) - UA_c (T_i - T_o) - \rho_a \phi_a L(X_i - X_o) = 0 \quad (2.4)$$

Where,

ρ_a: Density of air [kg m^{-3}]

$C_{p(air)}$: Specific heat capacity of air [J kg^{-1} K^{-1}]

Φ_a: Volumetric airflow rate [m^3 s^{-1}]

U: Overall heat transmission coefficient [W m^{-2} K^{-1}]

A_c: Greenhouse cover area [m^2]

L: Specific latent heat capacity of water [J kg^{-1}]

T_i: Temperature of greenhouse air [K]

T_o: Temperature of outside air [K]

X_i: Humidity ratio of inside greenhouse air [kg kg^{-1}]

X_o: Humidity ratio of outside air [kg kg^{-1}]

The internal temperature Ti, can be solved by solving the above equation provided the external climatic conditions and other parameters in the model are known. Huang et al. (2012) used an energy and mass balance governing equation to predict the inner temperature of the zones of their experiment. The equations are:

$$Cz\frac{dT_1}{dt} = C_{air}f_1\rho_{air}(T_{sa} - T_1) + C_{air}f_2\rho_{air}(T_{sa} - T_1) + \sum_{s=1}^{n} h_s A_s(T_s - T_1) + q_c \quad (2.5)$$

$$Cz\frac{dT_{1s}}{dt} = \sum_{s=1}^{n} h_s A_s(T_1 - T_s) + \sum_{s=1}^{n} h_s A_s(T_{out} - T_1) \quad (2.6)$$

Where,

Cz: Overall thermal capacity (kJ/C) of the zone

T_1 *and* T_2: Zone-1 temperature and zone-2 temperature respectively

T_{out} : Outdoor temperature

T_{sa} : Supply air temperature

T_s : Temperature of inside surface of the wall

C_{air}: The air density (kg/m^3)

ρ_{air}: Volume flow rate of the supply air (m^3/s)

f_2: Volume flow rate of the air between zone-1 and zone-2 (m^3/s)

h_s: Heat transfer coefficient for surface of the wall (W/m^2°C)

A_w: Area of the wall (m^2).

q_c stands for heat gain from unknown factors such as solar radiation, occupant, leakage of wall, etc.

Equations (2.5) and (2.6) illustrate that the rate of temperature change in Zone-1 is related to the dynamic variables such as: temperature difference between supply air and Zone-1, outdoor and Zone-1, Zone-2 and Zone-1. Huang et al. (2012) reiterated the fact that the

temperatures of the zones depend on the surface temperature of the walls, heat transfer coefficient of the walls, outdoor temperature, flow rate of the supply air, supply air temperature, solar gain and neighbouring zone temperature etc. The temperature distribution in each zone is assumed to be uniform, the density of the air and air-flow rates are both assumed to be constant. Defraeye et al. (2010) modelled the convective heat exchange at an exterior building surface, due to air flow along the surface, is usually modelled by convective heat transfer coefficients (CHTCs). The CHTC ($h_{c,e}$ - W/m²K) is defined as:

$$h_{c,e} = \frac{q_{c,w}}{(T_w - T_{ref})} \tag{2.7}$$

The CHTCs relate the convective heat flux normal to the wall $q_{c,w}$ (W/m²) to the difference between the surface temperature at the wall T_w (°C) and a reference temperature T_{ref} (°C), which is generally taken as the outside air temperature. The convective heat flux is assumed positive away from the wall. Temperature modelling is a challenging task due to its complexities (Huang et al., 2012). These complexities arise due to a variety of uncertainties that affect the time varying building's operational environment such as the occupant level, weather conditions, and the interactions of temperature of zones inside a building (Huang et al., 2012).

2.2.3 Heat Transfer Processes

The various heat exchange processes between a building and the external environment guide the derivations of the thermal modelling. The principles of heat transmission are on

the basis of heat conduction through materials and heat transfer from surfaces by radiation and convection (Barre et al., 1988). The rate of heat transmission through building materials depends on the characteristics of the material; its density, the size and arrangement of its particles or fibres, moisture content, temperature, and surface characteristics (Barre et al., 1988). Heat transfer obeys several laws. Amongst which are the basic laws of thermodynamics. A direct result of the first law is that everybody contains a discrete amount of internal energy; hence, the concept of enthalpy (Barre et al., 1988).

$$H = E + \frac{pV}{J} \tag{2.8}$$

Where E is the internal energy, p the pressure, V the volume and J the heat equivalent work. Heat continually moves due to different temperature potentials.

a. Heat Transmission Coefficient for Walls

The determination of the overall heat transmission coefficient is necessary if the wall is made up of different materials including air spaces and surfaces. The overall thermal resistance of the wall R can be represented as equals to 1/U. However, this applies only for steady state conditions of heat flow rate. The temperature drops at the two outer surfaces and through the wall components are

$$t_i - t_1 = QR_1 \tag{2.9}$$

$$t_1 - t_2 = QR_2 \tag{2.10}$$

$$t_2 - t_o = QR_3 \tag{2.11}$$

Where,

t_i and t_o: the indoor and outdoor temperatures.

t_1 and $t_{2:}$ the temperature readings at section 1 and 2 of a wall.

This can be rewritten in terms of the resistances, since the total temperature drop $t_i - t_o$ equals the sum of the temperature drops corresponding to the thermal resistances R_1, R_2 and R_3, and the heat Q is the same through each resistance, thus:

$$R = R_1 + R_2 + R_3 = \frac{1}{fi} + \frac{Lj}{kj} + \frac{1}{fo} \tag{2.12}$$

$$U = \frac{1}{R} = 1(\frac{1}{fi} + \frac{Lj}{kj} + \frac{1}{fo}) \tag{2.13}$$

f_i and f_o respectively, are the inside and outside heat transfer coefficients. *Lj* is the thickness of the *jth* layer and *kj* is the thermal conductivity of its material.

b. Surface Conductance

The rate of heat flow from a surface is affected by the temperature and the emissivity of the surface, air velocity, and the temperature difference between the surface and the air. The surface conductance *f* combines the effects of radiation, convection and conduction for a unit temperature difference between the surface and air. For inside surfaces f_i, when the air is still, it increases with the emissivity of the surface. For most design purposes,

the coefficient for outside surfaces f_o is approximated by selecting a wind velocity value (Barre et al., 1988).

c. Mean U coefficient of Multiple Walls

The mean U-coefficient for more than one wall, each with a different area and U-coefficient can be determined. The heat flow per degree temperature difference for each wall is A_1U_1, A_2U_2 and A_3U_3. The total heat flow per degree for all walls is simply the sum of the heat flow through each wall.

$$A_tU_m = A_1U_1 + A_2U_2 + A_3U_3 + A_4U_4 \tag{2.14}$$

Where A_t is the sum of the four wall areas.

However, if the wall has openings say windows for example, the thermal resistances of the openings differ from that of the wall. The combined flow according to (Barre et al., 1988) is:

$$AwUm = (Aw - Ao)Uw + AoUo \tag{2.15}$$

Where Aw is the gross area of the wall and Ao the area of the openings.

d. Conductivity of Homogenous Materials

The time rate of heat flow normal to a unit area in a homogenous material for a unit temperature gradient called the thermal conductivity, k is used. The thermal conductance C is the time rate of heat flow and gives the heat flow for the entire thickness of a material, being more general than the conductivity, which is a 1-in. thickness. Therefore, for

homogenous materials C = k/L, where L is the thickness of the material. For non-homogenous materials such as concrete building blocks, the thermal conductance is for the entire thickness.

e. Determination of Thermal conductivity

In determining the thermal properties of the green roof, the thermal conductivity of the different materials comprising the green roof must be found. Ondimu and Murase (2006) in their work to determine the thermal conductivity of the Sunagoke green roof plant stated that the material can be modelled as weighted average of the thermal conductivities of the different constituents of the green roof. Hence:

$$\lambda = \frac{\sum_{i=0}^{n} x_i \lambda_i}{\sum_{i=0}^{n} x_i} \tag{2.16}$$

Where x_i is given as $x_i = k_i v_i$ and is the weighting factor of constituent i.

λ_i is the thermal conductivity of constituent i in the element.

n is the number of constituents in each element

When the material is dry or saturated with water, $k = 1$.

f. Solar radiation gain

The solar radiation that goes into a building is given by:

$$Qr_{(in)} = Qr_{(out)} \times Tr \tag{2.17}$$

$Qr_{(in)}$: solar radiant energy into the building [w/m^2]

$Qr_{(out)}$: solar radiant energy outside the building [w/m^2]

Tr: Transmissivity of the wall material [w]

Nayak & Prajapati (2006) represented solar heat gain as:

$$Qi = \alpha s \sum_{i}^{m} A_i Sg_i \tau_i \qquad (2.18)$$

Where,

αs = mean absorptivity of the space

A_i = area of the i^{th} element (m^2)

Sg_i = daily average value of solar radiation (including the effect of shading) on the i^{th} element (W/m^2)

τ_i = transmissivity of the i^{th} element

m = number of elements

2.2.3.1 Conduction

Energy transfer via conduction can take place in solids, liquids and gases. This process happens when there is a transfer of energy from the more energetic particles of a substance to adjacent particles that are less energetic due to interactions between particles (Moran and Shapiro, 1995). Or simply, it is the process of heat transfer from one part of a body at a higher temperature to another (or between bodies in direct contact) at a lower

temperature (Eastop and MConkey, 1986). Conduction is quantified by Fourier's law that says heat flux is proportional to the temperature gradient in the direction of the outward normal.

Considering the transfer through, the basic equation of heat conduction is given by:

$$Q_{cd} = kA\frac{\Delta T}{D} \tag{2.19}$$

Q_{cd} : Quantity of heat flow/ Heat flux due to conduction [w]

k: thermal conductivity of the material [w/m/k]

A: Surface area [m^2]

ΔT: Temperature difference of the two media [k]

D: Thickness of the material [m]

Table 2.1 presents the values of thermal conductivity of different building materials.

Thermal diffusivity is also used to characterize heat flow through materials. It is the ability of a material to transfer thermal energy relative to its ability to store it. Thermal diffusivity which is related to thermal conductivity by:

$$\alpha = \frac{k}{\rho C} \tag{2.20}$$

ρ: density in kilogrammes

C: specific heat capacity in J/kgK

Table 2.1: Values of thermal conductivity of different materials (sourced from different literatures)

Material	**Thermal Conductivity (W/mK)**
Burnt brick	0.811
Mud brick	0.75
Dense concrete	1.74
Reinforced concrete	1.1
Lime concrete	0.73
Cement mortar	0.719
Cement Plaster	0.721
Timber (hardwood)	0.21
Timber (softwood)	0.13
Plywood	0.174
Sand	1.74
Glass	0.814
Air	0.026
Water	0.596
Copper	385
Aluminium	211
Soil (dry)	1.729
Soil (30% humidity)	0.93
Cultivated clay (25% moisture)	1.59
Sandstone	2.3

2.2.3.2 Radiation

This is the only heat transfer mechanism that does not require any medium of propagation (Long and Sayma, 2009) like convection and conduction because electromagnetic radiation travels through vacuum (Nayak and Prajapati, 2006). This is possible because it is able to pass through many gases, liquids and through some solids of relatively thin

layers of glass and plastic. Out of the electromagnetic spectrum, the thermal radiation is of importance to us as it is important in calculating solar gains and heat input into buildings from the sun. Long and Sayma (2009) gave the radiation exchange between two large parallel plane surfaces (of equal area A) at uniform temperatures T_1 and T_2 respectively, can be written as:

$$Q_{12} = \varepsilon_{eff} A\sigma(T_1^4 - T_2^4) \tag{2.21}$$

$$\varepsilon_{eff} = [\frac{1}{\varepsilon_1} + \frac{1}{\varepsilon_2} - 1]^{-1} \tag{2.22}$$

Q_{12} = net radiative exchange between surfaces (W)

σ= Stefan-Boltzmann constant ($5.67x10^{-8}$ $W/m^2\text{-}K^4$)

A = area of surface (m^2)

T_1 = temperature of surface 1 (K)

T_2 = temperature of surface 2 (K)

ε_1 and ε_2= Emissivities of surfaces 1 and 2 respectively

Nayak and Prajapati, (2006) noted the case of buildings' external surfaces such as walls and roofs are always exposed to the atmosphere and therefore subject to a different heat exchange. So the radiation exchange (Qradiation) between the exposed parts of the building and the atmosphere is an important factor. According to (Nayak and Prajapati, 2006) the heat exchange between the building surface and the sky is given by

$$Qradiation = A\varepsilon\sigma(T_s^4 - T_{sky}^4) \tag{2.23}$$

Where

A = area of the building exposed surface (m^2)

e = emissivity of the building exposed surface

σ= Stefan-Boltzmann Constant

T_s= temperature of the building exposed surface (K)

T_{sky}= sky temperature (K)

T_{sky} represents the temperature of an equivalent atmosphere. It considers the fact that the atmosphere is not at a uniform temperature, and that the atmosphere radiates only in certain wavelengths (Nayak and Prajapati, 2006). There are many correlations given to express sky temperature in terms of ambient air temperature (Nayak and Prajapati, 2006).

According to von Elsner (1983), for a clear (cloudless) sky:

$$T_{sky} = 1.2To - 21.4 \tag{2.24}$$

$$T_{sky} = 1.2To - 21.4 + 1(20.6 - 0.26To) \quad \text{Cloudy sky} \tag{2.25}$$

Where

T_{sky}: Sky temperature [°C]

T_o: Outside air temperature [°C]

For cloudy conditions, the sky temperature is given as:

$$T_{sky} = 1.2To - 21.4 + b(20.6 - 0.26To) \tag{2.26}$$

Where

b: cloudiness factor in the range 0 to 1 [-]

T_{sky}: Sky temperature [°C]

T_o: Outside air temperature [°C]

Nayak and Prajapati (2006) also equation in terms of the ambience temperature and radiative heat transfer coefficient:

$$Qr(c,sky)/A = hr(T_a - T_{sky}) + \varepsilon\Delta R \tag{2.27}$$

Where Ta = ambient temperature (K)

$$h_r = \varepsilon\sigma\frac{(T_a^4 - T_{sky}^4)}{(T_a - T_{sky})} \tag{2.28}$$

h_r is the radiative heat transfer coefficient, and ΔR is the difference between the long wavelength radiation incident on the surface from the sky and the surroundings, and the radiation emitted by a black body at ambient temperature. For horizontal surface, ΔR can be taken as 63 W/m^2 and for a vertical surface; it is zero (Nayak and Prajapati, 2006).

For building applications, usually convective and radiative heat transfer coefficients are combined to define surface heat transfer coefficient. Table 2.2 presents values of the surface heat transfer coefficient for a few cases.

Table 2.2. Values of surface heat transfer heat coefficient (Source: Nayak and Prajapati, 2006).

S/N	Wind Speed	Position of Surface	Direction of Heat Flow	Surface Heat Transfer Coefficient (W/m^2-K)
1	Still air	Horizontal	Up	9.3
		Sloping 45°	Up	9.1
		Vertical	Horizontal	8.3
		Sloping 45°	Down	7.5
		Horizontal	Down	6.1
2	Moving air 12 (km/h)	Any position	Any direction	22.7
	Moving air 24 (km/h)	Any position	Any direction	34.1

2.2.3.3 Convection

Heat transfer by convection, takes place at the surfaces of walls, floors and roofs. Convection can be described in two ways. It is either the transfer of heat from one part of a fluid (gas or liquid) to another part at a lower temperature by mixing of fluid particles (density differences) resulting in buoyancy (Larsen, 2006). Or, it can result from an external force such as a fan or wind. This is known as forced convection. According to Newton's law, convection can be given as:

$$Q_{cv} = h_c A \Delta T \tag{2.29}$$

Q_{cv}: Convective heat transfer/Heat flux due to convection [w]

h_c: heat transfer coefficient [w/m^2/K]

The heat transfer coefficient is often referred to as the convective conductance and as the film coefficient. Heat is imagined to be conducted through a thin stagnant film of fluid at the surface and then to be convected away by the moving fluid beyond (Long and Sayma, 2009). The numerical value of the heat transfer coefficient depends on the nature of heat flow, velocity of the fluid, physical properties of the fluid, and the surface orientation (Nayak and Prajapati, 2006).

2.2.3.4 Moisture Condensation in Walls

Condensation on the surface will occur whenever the dew point temperature of the room air is greater than the wall surface temperature (Barre et al, 1988). Garzoli (1985) gave the latent heat of condensation as:

$$Q_{cond} = \frac{h_{cvi} L (X_{air} - X_c)}{Cp_{(air)}} \tag{2.30}$$

Q_{cond}: Latent heat of condensation [w/m^2]

h_{cvi}: inside surface heat transfer coefficient of the cover [W m^{-2} K^{-1}]

$Cp_{(air)}$: specific heat of air [W h kg^{-1}K^{-1}]

L: latent heat of vaporization of water [W h kg^{-1}]

X_{air}: humidity ratio of air [kg kg^{-1}]

X_c: saturation humidity ratio for air at cover temperature [kg kg^{-1}]

2.2.3.5 Heat Flow through Fenestration Systems

The heat gains to the indoor air space through fenestration are the solar heat gain and the heat flow due to temperature difference between the indoor and outdoor temperatures. As solar radiation reaches the exterior surface of the fenestration (Io), parts of the incident radiation will be transmitted (It), reflected *(*Ir*)* and the rest will be absorbed *(*Ia*),* depending on the effective transmissivity (τ), reflectivity (ρ) and absortivity*(α)* properties of the fenestration system *(*$\tau + \alpha + p = 1$*)*(Tariku, 2008).

Tariku (2008) determined the heat gain through the fenestration system as the sum of heat flow through the fenestration system and a fraction of transmitted solar radiation which instantly heat the indoor air.

$$Qf = A_w U(T_e - T) + \frac{U}{h_o \alpha I_o} + f_{sa} I\tau \qquad (2.31)$$

Where:

A_w: window area

f_{sa} : Solar air factor

2.2.3.6 Evaporation

Evaporation term accounts for the sum of moisture addition to the indoor air due to evaporation of water from a reservoir (such as fish tank) and condensate surface. The evaporation rate is a function of the water temperature (or saturated vapour pressure), indoor air vapour pressure and airflow velocity in the zone (Tariku, 2008).

$$Qe = \sum A_e h_e (p_e - p) \tag{2.32}$$

A_e: surface area of the surface (m^2)

h_e: mass transfer coefficient for evaporation (kg/s m^2Pa)

p_e: saturated vapour pressure (Pa)

The above equation can also be rewritten in terms of the humidity ratio (described below)

$$Q_e = \frac{10^6}{6.22 \sum A_e h_e (w_e - w)} \tag{2.33}$$

The rate of cooling by evaporation (Q_{ev}) from, say, a roof pond, fountains or human perspiration, can be written as (Nayak and Prajapati, 2006):

$$Qev = mL \tag{2.34}$$

Where

m is the rate of evaporation (kg/s)

L is the latent heat of evaporation (J/kg-K)

2.2.3.7 Simplified Model of Heat Loss through Urban Buildings

Based on equations 2.9 to 2.34, the rate of heat loss through any building envelope element such as roof, wall or floor under steady state can be calculated, however, it is a cumbersome task due to the difficulty and inaccuracy in estimating the many parameters involved (Huang, 2012). Furthermore, it is not always obvious which mechanism will be

predominant, and indeed, more than one mechanism may be pertinent (Becker, 1986). The simplified model representing the heat loss through the building is given by:

$$Q_{f,r} = UA_c\Delta T \qquad [w] \tag{2.35}$$

A = surface area (m^2)

U = overall heat thermal transmittance (W/ m^2- K)

ΔT = temperature difference between inside and outside air (K)

2.2.3.8 Net Increase in Enthalpy of House Air

The difference between the net heat input into the building and the heat loss by ventilation, condensation and through the walls gives the net change in enthalpy of the building's air. This forms the basis of the indoor air temperature estimate.

2.2.3.9 Latent Heat

Latent heat refers to the energy absorbed or released during the change of phase in liquids or gases, such as during evaporation, condensation or transpiration. Latent heat transfer is based on vapour flow due to the vapour gradient between the surface and the air. The vapour potential is expressed as the actual content of vapour in the air on either a weight or volume basis (Ajwang, 2005).

2.3 Energy Usage in Buildings

2.3.1 Buildings and Climates

Across the continents, especially Sub-Saharan Africa, the climate of those regions are averagely hot for the most part of the year, subsequently causing higher indoor

temperatures in human dwellings. Although outside temperature might be difficult to individually alter, indoor temperatures in our houses are easy to modify to suit our comfort. Air conditioning systems are used to lower the indoor temperature to a more conducive one. These systems consume a lot of energy in their quest to lower or maintain the appropiate temperature that suits our comfort.

Buildings are the third highest energy consumers in the world. A majority of that energy consumed is used in heating or cooling our indoor environment, depending on the region and climate. Modifying the microclimate of our houses might not be mechanically easy or be undertaken on indivudal basis but interestingly, someone can modify the temperature of their inner spaces by controlling the amount of heat that comes into the buildings. Even from the first evidence of Neolithic houses and settlements, it is obvious that houses were not sited in a purely natural environment, but in a part of nature transformed according to a human plan (Benevolo, 1980).

Alexandri and Jones (2006) stated that with the evolution of human societies, settlements were transformed, evolved into villages, towns or cities, developed or faded away, according to the geographical, economic, social and cultural transformations taking place throughout time. They also mentioned that with the Industrial Revolution, urban spaces expanded dramatically, much faster and with much more significant changes than in their previous evolutionary periods.

2.3.2 Thermal Performance of buildings

The thermal performance of a building depends on a large number of factors. They can be summarised as (i) Design variables (geometrical dimensions of building elements such as walls, roof and windows, orientation, shading devices, etc.); (ii) Material properties (density, specific heat, thermal conductivity, transmissivity, etc.); (iii) Weather data (solar radiation, ambient temperature, wind speed, humidity, etc.); and (iv) A building's usage data, which are the internal heat gains due to occupants' behaviours, lighting and equipment, air exchanges, etc. (Nayak and Prajapati, 2006).

The interaction of a building with the external environment occurs in three ways; radiation, convection and conduction (Defraeye et al., 2010). A wall of a house interacts with the external environment with one side exposed to the outside environment and directly receiving solar radiation while the other side forming part of the indoor surfaces of the house. See Figures 2.1 and 2.2 for a pictorial presentation of the heat transfer process on a house. The total solar radiation incident on the outer surface of the wall is reflected back to the environment, while the remaining part absorbed by the wall and converted into heat energy. Another part of this is also lost to the environment through convection and radiation from the wall's outer surface. Again, the other part of this reaches into the room raising the indoor temperature and the rest is stored in the wall, thereby raising the wall surface temperature. This inner surface transfers heat by convection and radiation to the room air consequently raising its temperature (Nayak and Prajapati, 2006).

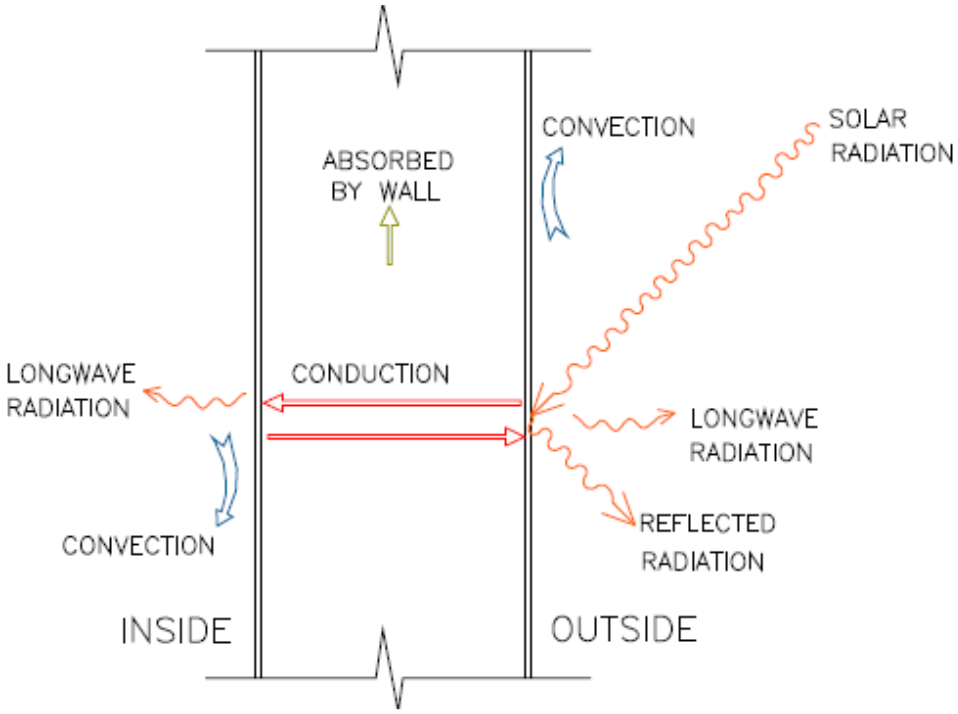

Figure 2.1. Heat transfer process occurring in a wall. (Source: Nayak and Prajapati, 2006)

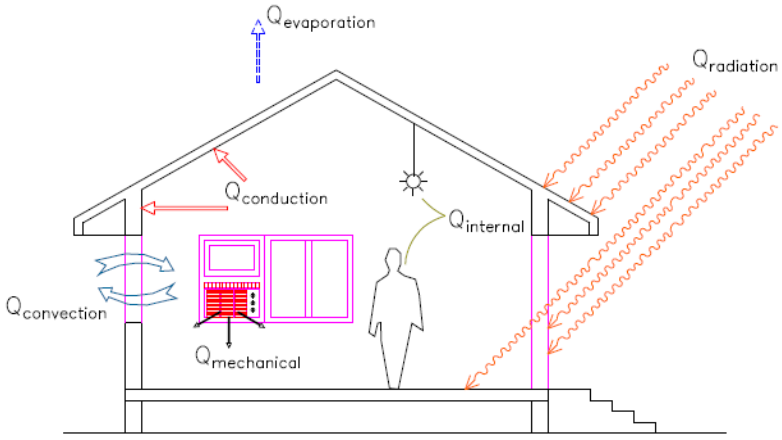

Figure 2.2. Heat exchange process between a building and the external environment (Source: Nayak and Prajapati, 2006)

The effect of buildings is considered as one of the main reasons for urban heat island phenomenom and building masses increase the thermal capacity, which has a direct bearing on the city temperature (Santamouris, 2012). Generally speaking, low and mid-latitude heat islands are unwanted because they contribute to cooling loads, thermal discomfort, and air pollution whereas high latitude heat islands are less of a problem because they can reduce heating energy requirements, however, this is a generalization; the actual impacts of urban climates and heat islands depend on the characteristics of local climates (Taha, 1997). The causes and effects of urban climates and heat islands are diverse and their interactions complex (Taha, 1997). They reduce wind speed and radiate heat through the building fabric and also in the form of air-conditioning equipment; the heat that is absorbed during the day by the buildings, roads and other construction in an urban area is re-emitted after sunset, creating high temperature differences between urban and rural areas (Santamouris, 2012).

In Hui (2007), a systematic approach focusing on two areas were examined in order to minimize the environmental impact of buildings through cooperation with external climate; the outdoor and indoor climate. Without careful consideration of the local climate, optimal building design and efficient building services operation would be difficult to ensure. The indoor climate includes temperature, relative humidity, ventilation and visual conditions. It focuses on the physical environmental conditions created inside built environments that provide for a comfortable and healthful experience, and that improve human performance and promote work productivity.

Results from meteorological simulations suggest that cities can feasibly reverse heat islands and offset their impacts on energy use simply by increasing the albedo of roofing and paving materials and reforesting urban areas and the simulations suggest that reasonable increases in urban albedo can achieve a decrease of up to 2°C in air temperature (Taha, 1997). With extreme increases in albedo, localized decreases in air temperature can reach 4°C under some circumstances and increases in vegetation in urban areas can result in some 2°C decrease in air temperatures (Taha, 1997). Under some circumstances, e.g. potentially evaporating soil-vegetation systems and favourable meteorological conditions, the localized decrease in air temperature can reach 4°C (Taha, 1997). The heat island intensity can result in up to 10 K temperature difference between the dense urban area and the surrounding rural zones (Santamouris et al., 2001).

2.3.3 Energy Consumption

Energy benefits vary mainly as a function of the climatic conditions and the characteristics of the building (Santamouris, 2012). Typically, peak summer indoor temperatures may decrease up to 2°C in moderately insulated buildings while cooling loads reductions may range between 10% and 40%. At the same time, the heating penalty may range between 5% and 10% as a function of the local climate and building characteristics. According to Akbari et al. (1992), for US cities with population larger than 100,000, the peak electricity load will increase 1.5–2% for every 1°F increase in temperature. In the findings of Castleton et al. (2010), about the possible energy savings for buildings in UK, they found out that most buildings in UK built to the 2006 UK

building regulations, having good roof insulation didn't record any substantial energy savings. Hence, only buildings with poor thermal insulations could profit more from green roofs.

Heating, ventilating and air conditioning (HVAC) systems in commercial buildings account for a large proportion of electricity bills for the buildings (Huang et al., 2012). Building Management Systems (BMS) provides building operators with a platform to monitor and record HVAC conditions as well as to tune the local control parameters with ease (Huang et al., 2012). An online predictive model incorporated with BMS is used for supervisory controls systems design (Huang et al., 2012). It offers the ability to track the long term dynamic behaviours of HVAC systems, by considering both the HVAC process and varying ambient environment (Huang et al., 2012). This model can be used for energy-efficiency control.

Jones (1985) stated how air conditioning is always related with refrigeration since when we talk of air conditioning; it is the cooling and dehumidification that is mostly talked about. Jones mentioned that refrigerants are responsible for the high cost of air conditioning. Aside increasing the individual cost of the equipment, it affects the general cost of cooling of a building when compared to heating a building. It is four times the cost of heating it. Conclusively, the need for air conditioning is not intentionally about cooling solely, but about providing a comfortable environment for human beings. This is so because of the sensible heat gains during summer and sensible heat losses in winter.

2.4 Vegetated Building Envelopes

2.4.1 Roles of Vegetation on Buildings

The trees and the open green spaces have multiple uses and their presence in the outdoors makes a major contribution to the saving of energy inside the buildings as well as to the improvement of the microclimate in the urban spaces adjacent to buildings and in urban subareas (Georgi & Dimitriou, 2010). The amount of energy needed for heating and cooling is decreased considerably by the suitable placement of trees around buildings, so that there is much shading from the sun during the summer and as little as possible during the winter (Georgi & Dimitriou 2010). According to Alexandri and Jones (2006), apart from creating outdoor conditions, which are more ‘‘human-friendly’’, from a thermal point of view, green roofs and green walls can also prove beneficial for indoor thermal conditions. In addition to the fact that they add a further insulation layer to the building’s fabric, they can decrease cooling load demands inside the building quite significantly due to the microclimatic modifications. Mitigation techniques aim to balance the thermal budget of cities by increasing thermal losses and decreasing the corresponding gains (Sanatamouris, 2012). In general, green roofs and green walls cool the microclimate around them, which can lead to quite important energy savings for cooling, depending on the climatic type, the amount and position of vegetation on the building (Alexandri and Jones, 2006).

2.4.2 Green Roofs

Roofs present a very high fraction of the exposed urban area (Santamouris, 2012). Given that the available free ground area in the urban environment is quite limited and of very high economic value, it is relatively difficult to implement large scale mitigation technologies on the ground surface of cities. At the same time, urbanization decreases the proportion of spaces dedicated to plants and trees or other mitigation infrastructures because of new building developments (Mathieu et al., 2007 as cited in Santamouris, 2012). On the contrary, roofs provide an excellent space to apply mitigation techniques, given that the relevant cost is limited, while the corresponding techniques are associated to important energy savings for the buildings.

Zinzi (2010) (as cited in Santamouris, 2012) mentioned that there are two major techniques in which mitigation technologies are associated with roofs, either by planting vegetation, called living or green roofs or by using roofing materials of high albedo property also called cool or reflective roofs. Both technologies can lower the surface temperatures of roofs and thus to decrease the corresponding sensible heat flux to the atmosphere (Santamouris, 2001). In (Santamouris et al., 2011), green or living roofs are partially or fully covered by vegetation and a growing medium over a waterproofing membrane. The two main classifications of green roofs are intensive and extensive green roofs. They are differentiated based on the depth of growing media and weight. Extensive green roof has a low depth of growing medium. See Figure 2.3 for an image of the composition of a green roof. Typical vegetation types grown on extensive roof are lawn

or sedum; generally, low rising plants. While intensive green roof have deeper growing layer and heavy in structure. Due to the deep growing layer, shrubs and trees can be grown on it (Sailor, 2008).

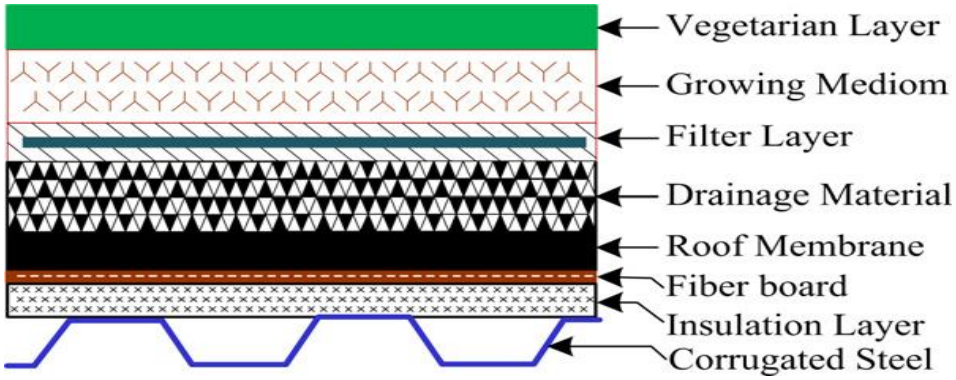

Figure 2.3 Components of a green roof over corrugated steel roof (Saadatian et al., 2012)

Green roofs present a variety of advantages like storm water runoff management, increased roof materials durability, decreased energy consumption, possible better air quality and noise reduction, offer space for urban wildlife and increased mitigation of urban heat island (Santamouris et al, 2012). Cool or reflective roofs are typically white and present a high albedo. Products used in cool roofs are single ply or liquid applied (Mac Cracken, 2009). Typical liquid applied products involve white paints, elastomeric, polyurethane or acrylic coatings. Examples of white single ply products involve EPDM (Ethylene-Propylenediene-Tetrolymer Membrane) PVC (Polyvinyl Chloride), CPE (Chlorinated Polyethylene), CPSE (Chlorosulfonated Polyethylene), and TPO (Thermoplastic Polyolefin) materials (Mac Cracken, 2009).

A review of the recent developments on the field of liquid applied materials used in reflective roofs is given in Santamouris, Synnefa and Kalissi (2011). The first generation of materials used in cool roofs consisted of natural materials quite easily found in nature characterized by a relatively high albedo, rarely higher than 0.75, while the second generation was based on the development of artificial white materials designed to present very high albedo values close or higher than 0.85. In a later third phase of development, coloured high reflective materials have been developed. The overall idea was to develop coloured materials presenting a high reflectivity value in the infrared spectrum. The specific materials were characterized by a much higher global reflectivity than the conventional ones of the same colour and were associated to important energy savings when used in building roofs or urban infrastructures (Santamouris, 2007). Quite recently, fourth generation reflective materials based on nanotechnological additives like thermochromic paints and tiles, or PCM doped cool materials have been developed and likely to be used for future cool roof applications.

Santamouris (2012) mentioned the specific energy benefits depend on the local climate, the green roof design and more importantly on the specific building characteristics, given that in green roofs heat transfer benefits are mainly provided through latent heat processes, the performance of the system is higher in dry climates. However, he mentioned again that the building characteristics also define the possible contribution of green roofs. In non-insulated buildings the impact of green roofs is much higher than in insulated ones. It is evident that the better the insulation of the roof, the lower the

contribution of the green roof. In parallel, the characteristics of the energy load of the building define the specific contribution of the roof system (Santamouris, 2012).

According to Santamouris (2001), in buildings presenting a high part of their energy load because of the ventilation gains or losses, internal or solar gains, green roofs have a limited contribution. On the contrary, in buildings where the energy load is due to the heat transfer though the opaque parts of the envelope, vegetative roofs may contribute significantly to reduce heating and cooling loads. Existing studies performed for various types of buildings, green roof characteristics and climatic zones, show that expected reduction of the annual energy load may vary between 1% and 40% in extreme cases. In reality, in well insulated modern buildings the energy contribution of green roofs is quite modest (Santamouris, 2012).

Lui and Minor (2005) in their experiment- 2 green roofs with 75mm and 100mm of lightweight growing medium, in Canada- found that heat gain through green roofs was reduced by an average 70-90% in the summer and 10-30% in the winter. In Florianopolis (Brazil), a temperate region, Parizittio and Lamberts (2011) found out that green roofs reduce heat gain by 92-97% compared with ceramic and metallic roofs. Meanwhile Riyadh showed 90% cooling load decrease, Montreal 85%, Mumbai 72% decrease, Athens 66% and Beijing 64% (Alexandri and Jones, 2008).

The intial cost of green roofs is more than three to six times of a conventional roof (Saadatian et al., 2013). However, a lifecycle assessment of a green roof compared with a bare roof has shown that there are economic savings from using greeen roofs. Green

roofs improves the life of roofs by elongatng it and protecting it from harsh weather conditions. It saves energy from manufacturing a green roof and from heating or cooling loads.

2.4.3 Green Walls

Whereas green roofs have been actively promoted in many cities, green walls (referring to walls covered by vegetation in the sense of building engineering and building physics) have received less attention (Jim and He, 2011). The vegetative shield provides an additional barrier between the building interior and the hot (or cold) external environment. It is important to explore quantitatively vegetation–atmosphere interactions in addressing solar energy transmission through the atmosphere to the vegetation canopy (Chen et al., 2007).

Various factors influence energy exchange and transmission of a vertical greenery (referring to walls covered by vegetation in the sense of ecological functions in an ecological system) ecosystem, such as weather condition, plant physiological function, and building structure (Jim and He, 2011). Wang et al. (as cited in Jim and He, 2011) mentioned that the amount of energy absorbed by an ecosystem is governed by the biophysical properties of the vegetation canopy (referring to the upper surface of vegetation), and the driving potentials established by temperature and humidity gradients between the surface and the atmosphere. Partitioning of the incoming radiation into vegetation canopy absorption, transmission, reflection and transformation of absorbed

energy help to understand the interactions between solar energy and plants (Jim and He, 2011).

Quantitative assessment of the interactions between solar radiation and vegetation canopy demands specification of variables that determine radiation transport through the vegetation canopy. These variables include intrinsic canopy properties such as absorption, reflection and transmission from the atmosphere into the canopy. The canopy radiation regime is a function of the optical properties of individual leaves and ground surface under the canopy and canopy structure. This feature of the shortwave energy conservation in vegetation canopy provides powerful means for accurate specification of changes in canopy structure (Jim and He, 2011).

However, the solar radiation transmission model for vertical greening has not been attempted. Greenery on buildings is a combination of natural vegetation and artificial structures, incurring marked differences from natural conditions. Vegetation covering a building could induce cooling of indoor space by reflecting and absorbing solar radiation, cooling by evapotranspiration, enhancing insulation, and acting as shade (Jim and He, 2011).

CHAPTER 3

MATERIALS AND METHODS

3.1 Experimental Setup

The experimental setup for the study considered a number of design variables; material properties, weather conditions and building usage data while setting up. A detailed description of the location and the physical models built for the study are elaborated in the proceeding sections. The experiment was required in order for us to achieve all the specific objectives. The data to be obtained from the set-up will be used will be used to validate the model that will be developed, then another set of data will be used to correlate the predicted values and values obtained from the model. Another set will be used to adequately evaluate the effect of the living green roof on the cooling loads of urban buildings and on indoor microclimate. And lastly, another set of data will be used to compare the indoor microclimates of the urban building with green roof and the bare roof building. Two rooms like urban house were erected in order to measure microclimatic data to be used for the study.

3.1.1 Location of the Study

The field experiments were located at Jomo Kenyatta University of Agriculture and Technology, Juja campus, Kenya, which represented an urban like area, complete with paved areas, concrete buildings and asphalted roads. The place is located in Central Kenya, an equatorial high altitude region on latitude 1° 11’ 00” S and longitude 37° E 07’ 00” with an altitude of 1416m (4648ft) above sea level (Kenya, 2013). The two models

were located between two blocks, about 5 metres and 10 metres from each office block. This positioning replicates a location of a house in a typical urban environment, densed with building developments. There is about 5 metres of space between the two models. The landscape of the models was partially covered with a native grass. One model served as the model under observation, while the other served as the control. After a month of obtaining data, the roles between the two models were switched in order to assess whether the influence of one of building's proximity to the other building had a significant effect or not. See Figures 3.3 and 3.4 for a pictorial view of the physical models. Many researches in the field of indoor monitoring of temperatures obtained data for about 9 days, 14 days or more. Hence, a data collection of a month will provide adequate data to ascertain findings.

Figure 3.1. The two models observed for the experiment

Fig. 3.2a

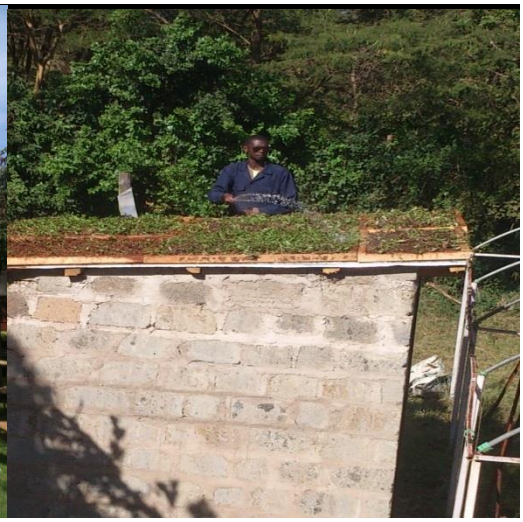

Fig. 3.2b.

Fig. 3.2c

Fig. 3.2d

Figure 3.2 The different views of the field scale model (a) The full model. (b) The vegetation boxes on the roof. (c) The door. (d) The single glazed window (on opposite side of the door).

3.1.2 Model Description

Two physical models having the same geometric and material properties were constructed. Stones, which are commonly found and used for construction within the locality were used to construct the buildings. The foundation was 200 mm deep without any column footings. The floors of the rooms were decked with murram, stone ballast and thereafter a fine finish of cement mortar was made on the surface. Polyethylene was used below the floors and around the perimeter of the floor to prevent moisture rise in the rooms. The inside wall surfaces, with the exclusion of the outside surfaces, were finished with cement mortar. A conventional roof was made, slanting in one direction, about 26°, covered with gauge 30 Aluminium roofing sheet. There is a single door and window for each model, located in opposite direction and against the sun path. The door was made with timber while a single glazing window was used. No ceiling was constructed because houses with green roofs are normally decked and left bare from below inside the buildings. In essence, these represent the exact construction procedure of a building in the locality. See Figure 3.3 for the structural drawings of the models.

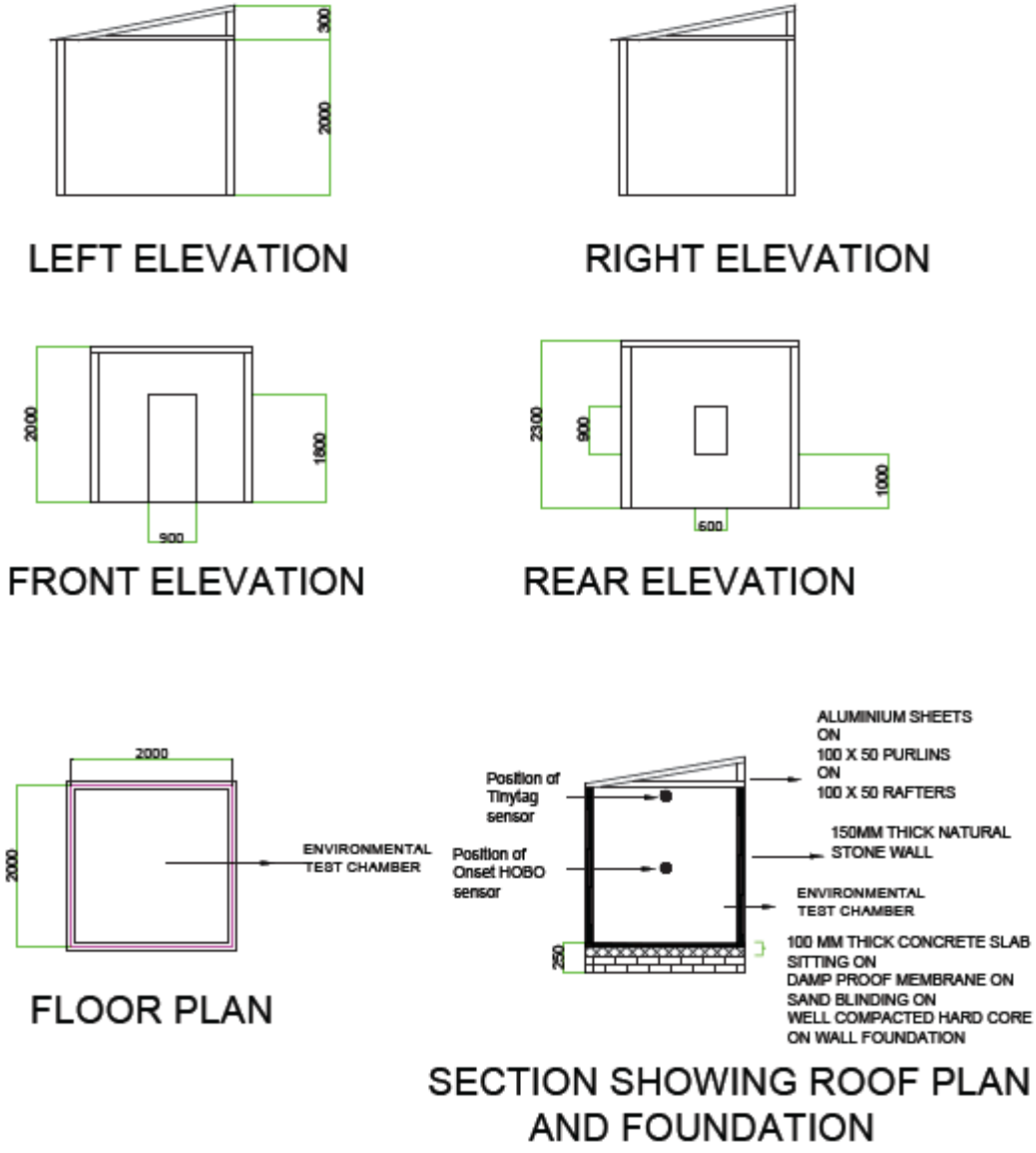

Figure 3.3 Sketches showing the different views of the field model in AutoCAD

3.1.3 Construction of Green Roof

Boxes about 100mm deep were made with the same corrugated iron sheet used on the roofing of the structure and timber, such that, the top of the box was open. The corrugated

sheet lying below was perforated in order to aid drainage of the green roof. A soil layer was later added about 90mm in depth to serve as the growing media of the vegetation used. 6 boxes were made that covered the entire roof area when placed on top of the model.

3.1.4 Instrumentation

3.1.4.1 HOBO U30 NRC Station

HOBO onset instruments will be used for collecting data for the study. All data valus were obtained at an interval of 10 minutes. See Figure 3.4 for an image of all the sensors installed on site. Adrian et al. (2013) used HOBO instruments in their research in predicitng the envelope performance of commercial office buildings in Singapore. The logger recognises Smart Sensors plugged into the logger and collects data about various parameters. The connections between the Smart Sensors and the logger are digital, ensuring accurate, reliable data collection and storage. It has a normal operating range of -20 to 40°C but it can operate outside the normal range, only to the detriment of the battery service life. It has a 0 to 2 seconds for the first data point and +/- per week at 25°C. All sensors from Onset HOBO logged their values into the logger. The logger together with other sensors (for outdoor temperature/RH, solar radiation, wind speed and wind direction) were mounted on a tripod mast. The three meter mast (M-MPA) was bolted on a slab 3 metres above the ground. This height places it in a good position to measure wind and solar radiation. All data logs into the logger from the 6 sensors (4 as mentioned above

and 2 placed inside the two field models) and is downloaded via computer software called HOBOware, from Onset HOBO, the manufacturers of the sensors.

Figure 3.4 Image of Onset HOBO weather station, installed with sensors (wind vane and anemometer, solar pyranometer, temp & RH) and a U30 NRC logger, standing on a 3m high concrete slab.

3.1.4.2 Solar Radiation

Solar radiation was measured using the Silicon Pyranometer smart sensor (S-LIB-M003), designed to work with the OnSet HOBO Weather Station logger. All calibration parameters are stored inside the smart sensor, which automatically sends information to the logger without any need for extensive setup or programming. It has a measuring range between 0 to 1280 W/m^2 and a spectral range between 300 to 1100nm. Its accuracy is within +/-10 W/m^2 or +/-5%, whichever is greater in sunlight. It has an additional temperature induced error of +/-0.38 $W/m^2/°C$ from +25°C. Angular accuracy is cosine corrected between 0 to 80° from vertical; Azimuth Error <+/-2% error at 45° from vertical, 360° rotation. It has a resolution of 1.25 W/m^2 and a drift of <+/-2% per year. Readings were taken at 10 minutes interval. The sensor is placed on the mast described above, almost 7m above ground level.

3.1.4.3 Wind Speed

Wind speed was measured using Wind Speed smart sensor (S-WSA-M003), designed to work with OnSet HOBO station loggers. All sensor parameters are stored inside the smart sensor, which automatically communicates configuration information to the logger without the need for any programming or extensive user set-up. The measurement range is 0-45m/s with accuracy of +/-1.1m/s or +/-4% of reading (whichever is greater). It has a resolution of 0.38m/s. Gust is measured at a highest 3-second gust during the logging interval. Operating temperature range is between -40 to 75° C. The sensor is composed of a three-cup polycarbonate anemometer housing measuring 41*16cm. It records

average wind speed over a logging interval of 10 minutes. The anemometers are placed on the mast described and shown above, at about 7m height from the ground level.

3.1.4.4 Wind Direction

Wind direction of the wind speed measured above was also recorded using the Wind Direction smart sensor (S-WDA-M003), also designed to work with OnSet HOBO station loggers. All sensor parameters are stored inside the smart sensor, which automatically communicates configuration information to the logger without the need for any programming or extensive user set-up. The measurement range is 0 to 355°, with an accuracy of +/-5° and starting at a threshold of 1m/s. Its maximum wind speed survival is 60m/s. It has a turning radius of approximately 13.5 cm. Each wind measurement is calculated every three seconds for duration of logging 10 minutes interval. The wind vane is situated on the mast described and shown in Figure 3.4.

3.1.4.5 Air Temperature and Relative Humidity

Due to unavailability of only a complete set of HOBO onset thermal sensors, another thermal sensor from a different manufacturer was used to carry out the measurement of indoor temperatures and relative humidity. In total, there were 5 sensors recording both temperature and relative humidity at the same time. One sensor deployed outside taking the outdoor temperature and relative humidity and two others, measuring the indoor temperature and relative humidity in both field models were placed equidistant between the roof and floor. All three mentioned above are from OnSet HOBO manufacturer. The other 2 (from Tinytag) were placed just below the roofs inside the two models. The

measurement that was used for model validation and prediction were from HOBO. While the measurement from Tinytag instruments were only used in analysing and discussing temperature differences below the green roof and the bare roof. A statistical test was carried out between the data obtained from the two sensors. Result showed that there was no significant difference between the measurements from the two different sensors.

a. OnSet HOBO Temperature and RH Sensors

The Temperature/RH smart sensor (S-THB-M008) is designed to work with smart sensor-compatible HOBO data loggers. All sensor parameters are stored inside the smart sensor which automatically communicates information to the logger. For temperature readings, it has a measurement range between -40 to 75° C with an accuracy of +/-0.21°C from 0 to 50°C. Its resolution is 0.02° C at 25° C and a response time of 5 minutes in air moving 1m/sec. It has a drift of < 0.1°C per year. All measurements were taken at 10 minutes interval.

For the RH readings, it has a measurement range between 0 to 100% at -40°C to 75°C. It has an accuracy of +/-2.5% from 10% to 90% RH (typical), to a maximum of 3.5% including hysteresis. It has a resolution of 0.1% RH at 25C and a drift of <1% per year typical. All measurements were taken at 10 minutes interval. The sensor is placed on the mast described and shown above.

b. Tinytag Temperature and RH Loggers

Elias-Ozkan et al. (2006) used it in their research in comparing the different thermal properties of building materials in Turkey. The indoor temperature and relative humidity

data logger (TGU-4500) has a measurement range between -25 to 85°C and 0 to 95% RH using built in sensors. It is primarily suited to indoor use. It has an operating range between -40°C to 85°C monitoring. It has a resolution of 0.01°C or better and a response time of 20 minutes to 90% FSD in moving air. For RH, it has an accuracy of +/-3% at 25°C, a response time of 10 seconds to 90%. All measurements for both the temperature and RH were taken at 10 minutes interval. Measurements recorded in this logger are collected via the computer software, Tinytag explorer. The logger is placed in the two rooms as shown in the diagram above.

3.2 Modelling and Simulating Green Roofed Urban Building Indoor Microclimate

3.2.1 Modelling of GRUBCLIM

The term energy balance is used to refer to the mathematical analysis of the gains, losses and storage of energy by an object. Thermodynamically, temperatures of objects or zones can be determined through an energy balance equation. This can be achieved by taking into consideration the known temperatures of all the objects or processes which interact with the object or zone. A new Green Roofed Urban Building Microclimate model called GRUBCLIM is developed in this study via energy balance. It is arrived at by considering the building as a system exposed to local weather conditions such as wind, solar radiation and rainfall on its outside and internal heat gain via the envelope and fenestration systems. These microclimatic parameters were identified as implicit for us to properly capture the thermodynamic behaviour of the green roofed urban building (GRUB). GRUBCLIM is

expected to predict to indoor air temperature of urban houses with living green roof. Considering the building envelope, the basic ways in which heat exchange occurs for the field scale model are through the green roof, walls, floor and the fenestration system. A flowchart of GRUBCLIM is shown in Figure 3.5.

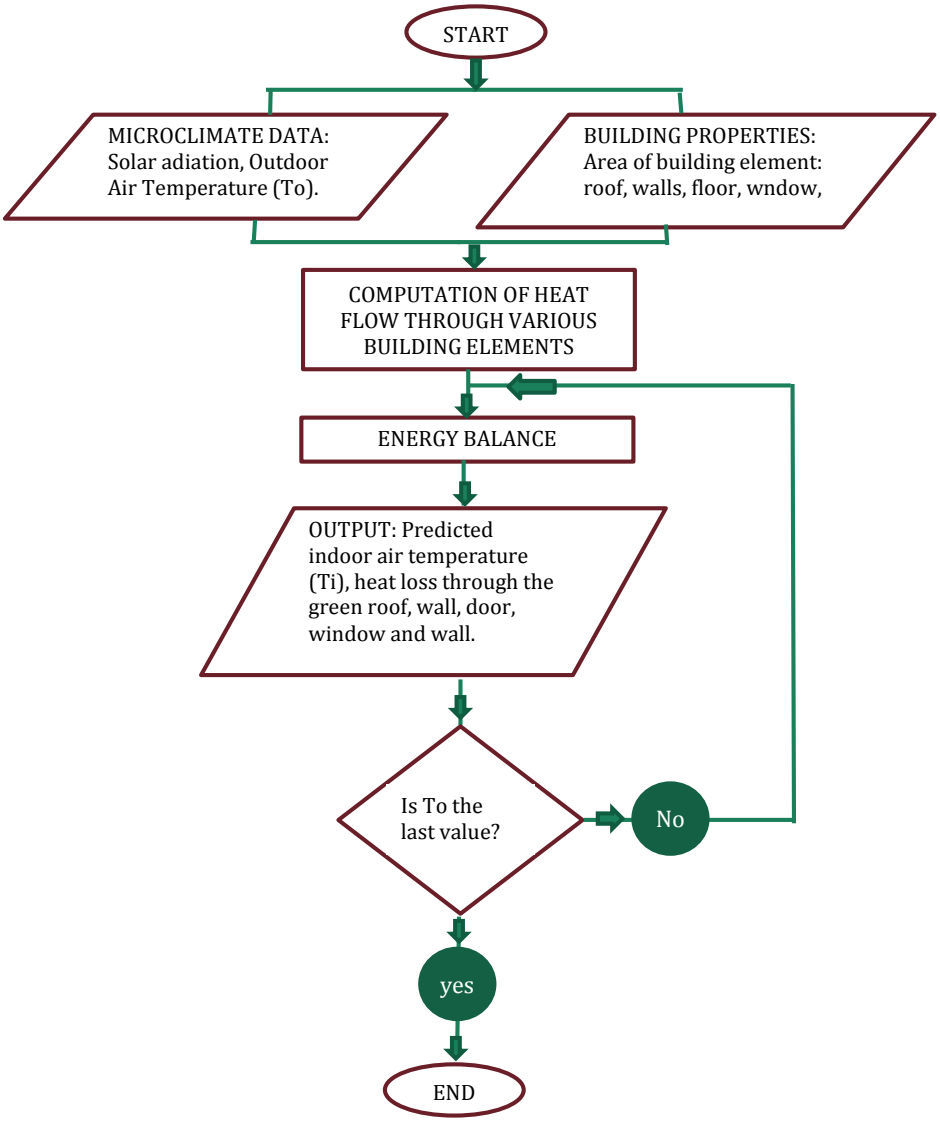

Figure 3.5 Flowchart of GRUBCLIM

A basic assumption made is that the indoor air of GRUB is uniformly mixed; hence, the energy balance for the urban building with a green roof can be generalized as:

$$Q_T = Q_W + Q_F + Q_G + Q_R + Q_D \tag{3.1}$$

Where,

Q_T: Total energy that comes into the house [w]

Q_W: Energy loss through the walls [w]

Q_F: Energy loss into the floor [w]

Q_G: Energy loss through the glazing (window) [w]

Q_R: Energy loss through the green roof [w]

Q_D: Energy loss through the door [w]

$Q_{T\,is}$ calculated by multiplying the total solar radiation that comes into the building by the floor area of the house. All other parameters in the above equation (3.1) can be substituted with equation (2.35), which uses the overall heat transfer coefficient (U) of heat transfer. Thus:

$$Q_T = U_W A_W \Delta T + U_F A_F \Delta T + U_G A_G \Delta T + U_R A_R \Delta T + U_D A_D \Delta T \tag{3.2}$$

Where,

U: overall heat transmission coefficient [W m^{-2} K^{-1}]

A: building surface area [m^2]

Ti: temperature of indoor air [K]

To: temperature of outside air [K]

For each building element that comprises of different materials, such as the wall and the roof, the overall U-value is arrived at using equation (2.13). All single U-values of materials were taken from literature quoted in Table 2.1. See Table 3.1 for the values of thermal properties used. To predict the indoor air temperature (*Ti*), equation (3.2) is solved provided the external climatic parameters measured (solar radiation and outside temperature).

Table 3.1 Thickness, thermal conductivity and U-value of different materials used for the analysis

S/N	Element	Composition	Li (m)	Kj(w/m-K)	Li/Kj	1/hi +1/ho	Rt	U
1	Wall	Plaster	0.05	0.721	0.0693481	0.149807	0.28437	3.51651
		Stone	0.15	2.3	0.0652174			
					0.1345655			
2	Door	Timber	0.05	0.21	0.2380952	0.149807	0.3879	2.57797
3	Window	Single glazing	0.01	5	0.002	0.149807	0.15181	6.58731
4	Floor	Plaster	0.05	0.721	0.0693481	0.149807	0.27738	3.60511
		DPC	0.1	1.74	0.0574713			
		DPM	0.00025	0.33	0.0007576			
					0.127577			
5	Roof	Plants			0.5	0.136852	0.69975	1.42908
		Soil layer	0.1	1.59	0.0628931			
		Veg box	0.00025	105.9	2.361E-06			
		Roofing	0.00025	105.9	2.361E-06			
					0.5628978			

*Calculated based on manufacturer details.

3.2.2 Validating GRUBCLIM

Data obtained between 28th April and 18th May will be used to validate the model. The data is obtained from the field model further away from the office block because the effect of greening is thought to be more pronounced in that building. However, later objective to be achieved when comparing the indoor microclimates of the two houses will prove the hypothesis right or wrong. Validation of the model is necessary in order to train the model and to see how it correlates to the data.

3.2.3 Simulating GRUBCLIM

GRUBCLIM is modelled in SIMULINK, a module in MATLAB. The inputs of GRUBCLIM are outdoor air temperature and solar radiation (all measured just outside the field model). The GRUBCLIM simulation model masks various subsystems. Each subsystem does a different function and returns the output.

The tasks performed in the SIMULINK model are:

Reading Input File: The input is the weather data collected at the field model site, i.e. Outdoor air temperature, indoor air temperature and global solar radiation. The measured indoor air temperature is comparison purposes with the predicted values from the GRUBCLIM only.

Computations: The following computations are done: calculation of heat loss through the roof, calculation of heat loss through the walls, calculation of heat loss through the window, calculation of heat loss through the door, calculation of heat loss through the

floor, calculation of energy balance and prediction of indoor air temperature. See Figure 3.6 for the block diagram of the energy balance in SIMULINK.

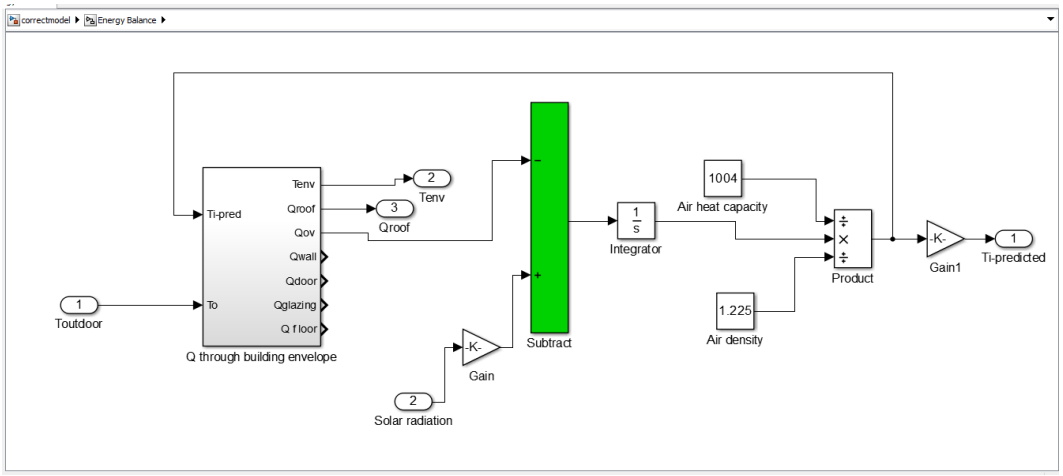

Figure 3.6. Block diagram of the energy balance in SIMULINK

Other constant parameters used in the model are:

Specific heat capacity of air: 1004 J/kg/K,

Density of air: 1.225 kg/m^3,

The model outputs include the following parameters:

Predicted indoor air temperature [°C].

Heat loss through the roof [W].

Heat loss through the Window [W].

Heat loss through the door [W].

Heat loss through the floor [W].

Heat loss through the walls [W].

Computations: The following computations are done

- Calculation of heat loss through the roof

- Calculation of heat loss through the walls

- Calculation of heat loss through the window

- Calculation of heat loss through the door

- Calculation of heat loss through the floor

-Calculation of energy balance and prediction of indoor air temperature

The constant parameters used in the model are:

- Overall heat transmission coefficient (U-value):
- U-value of roof (30% moisture, soil, plants, roofing sheet):
- U-value of wall (natural stone and plaster):
- U-value of cement plaster:
- U-value of building stone:
- U-value of single window glazing:
- U-value of door (timber):

The model outputs include the following parameters:

a. Predicted indoor air temperature [°C].
b. Heat loss through the roof [W].
c. Heat loss through the window [W].

d. Heat loss through the door [W].

e. Heat loss through the walls [W].

Data obtained between 18th May and 5th June will be used to simulate the model. Thereafter, the predicted values will be compared with the measured values to see the correlation. Similarly, the data for simulation was also obtained from the same house the data for validation was obtained from.

3.3 Evaluating the Effects of Green Roof on Cooling Loads

After the set-up is up and running, data obtained between 18th May and 6th July will be used to evaluate the influence of green roofing on cooling loads. The field scale models constructed and observed for microclimatic differences had no effect of ventilation system added to them. Alexandri and Jones (2008) in their research to determine energy savings from green walls and roofs in an urban canyon used a steady state analysis in determining the amount of heat gains and losses (q_E) from a building fabric using equation 3.3:

$$q_E = U(T_{out} - T_{in}) \tag{3.3}$$

Where U is the average U-value of the building's fabric, T_{out} is the outdoor temperature and T_{in} is the indoor temperature. However, this analysis used a general U-value and only considered the effect of the microclimatic conditions. In this study, a similar analysis was done in arriving at the amount of heat gains and losses from the field models. The different U-values of the two models were considered. An average U-value of 3.54 was used for GRUB while 4.72 was used for BRUB. The microclimate difference was arrived

by choosing 23°C (based on ASHRAE Comfort Standard 55-74) to serve as the comfortable indoor temperature (T_c), then subtracted from the indoor temperature of the two models as shown in equation 3.4:

$$q_{E[GRUB]} = U_{GRUB}(T_{GRUB} - T_C) \tag{3.4}$$

Similarly, for the bare roofed urban building:

$$q_{E[BRUB]} = U_{BRUB}(T_{BRUB} - T_C) \tag{3.5}$$

Only temperature readings above 23°C will be used for the evaluation.

3.4 Comparing the Indoor Microclimates of Green Roofed Urban Buildings and Bare Roofed Urban Buildings

For effective conclusions to be reached on the effect of green roofs, a comparison is needed between the house with the living green roof and the house with a conventional roof. Sensors were both placed inside the two houses at two different locations. One sensor was positioned just below the roof and the other sensor placed equidistant between the roof and floor. Data to be used for comparison is obtained between 28th April and 6th July. However, in this case, both daytime and night time values of temperature and relative humidity will be used. The green roof was first of all placed on the building further away from the office block. Data was obtained between 28th April and 4th June. Thereafter, the green roof was placed on the model closer to the office block and data was obtained from 5th June to 6th July.

CHAPTER FOUR

RESULTS AND DISCUSSONS

4.1 Model Validation

GRUBCLIM was developed in order to predict the indoor air temperature of GRUB. In order to measure the actual significance of the GRUBCLIM, a validation process was carried out. The process compares the predicted values from GRUBCLIM and compared against measured temperature. The model was validated using the microclimatic data obtained at the field scale model site. The validation data was measured from 28th April to 18th May, 2014. Thereafter, the model was simulated and compared against another set of data obtained between 18th May and 5th June, 2014. The best representatives of the data for the research were those obtained between 9.00am and 4.00pm, when the effect of the solar radiation is thought to be highest. During that period, the minimum ambient temperature recorded around the field scale model was 8.42°C while the maximum was 30.52°C.

4.2 Model Simulation

Figure 4.1 compares the predicted indoor air temperatures from GRUBCLIM and the values obtained during the experiment. From the figure, it can be seen that the predicted values are in good agreement with the measured values. The model has a correlation coefficient of 0.885. See Figure 4.2 for the correlation between the predicted and observed values. The highest temperature value observed was 22.64°C against the highest predicted by the model at 22.08°C. Similarly, the lowest temperature predicted is 15.78°C against

the measured value of 17.65°C. The highest difference recorded between the two values is 3.58°C. These differences can be attributed to the standard error of 0.0529 of the predicted values. Generally, GRUBCLIM over predicts during the daytime and under predicts during the night.

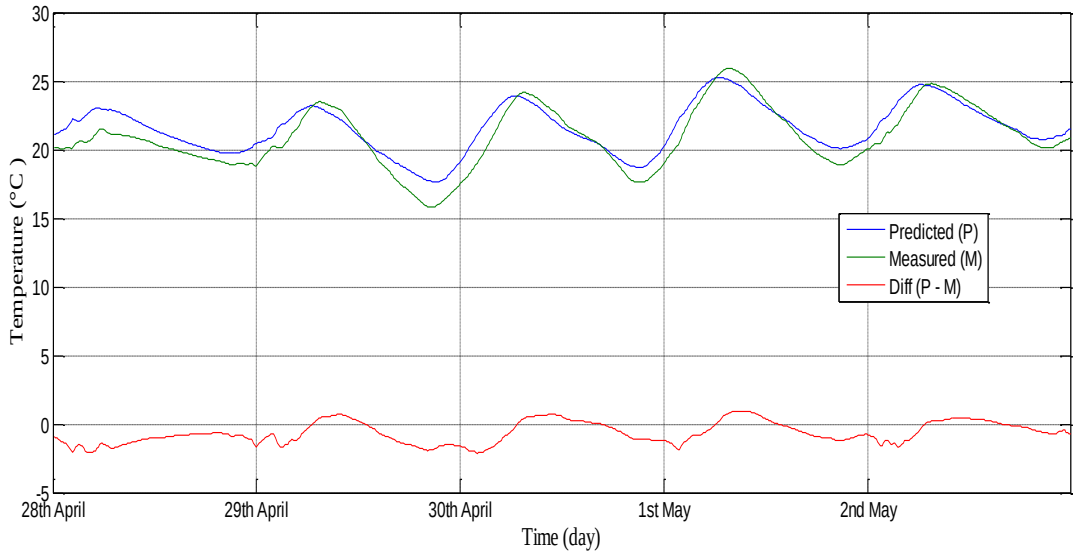

Figure 4.1 Relationship between the predicted air temperature from GRUBCLIM, the measured value and the difference at each point of the two values.

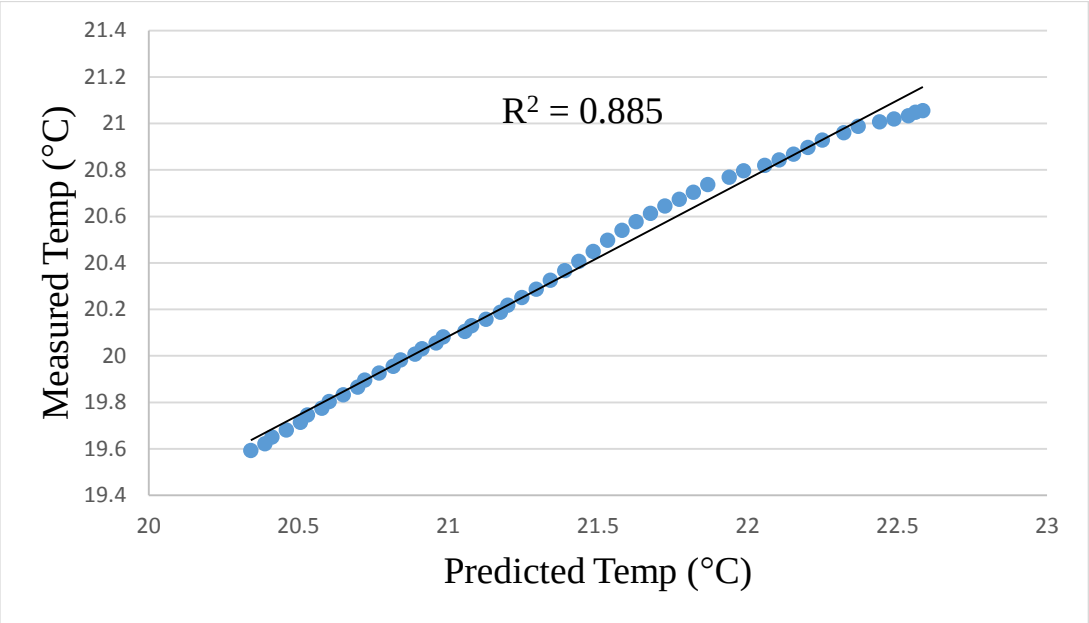

Figure 4.2. Correlation between the predicted temperature values of GRUBCLIM and measured values.

Figure 4.3 shows the predicted, measured and outdoor temperature readings plotted together, thus, showing possible reason of under and over prediction of GRUBCLIM. It can be seen that during the daytime, when the outdoor temperature is higher than the indoor temperature, GRUBCLIM under predicts. Conversely, during the night time, when the outdoor temperature is below the indoor temperature, GRUBCLIM over predicts. A z-test was carried out to compare the differences between the measured and the predicted temperature values. Results showed that there is a significant difference (means difference 0.563) between the measured and predicted values. The analysis returned a p-value of 1.11022E-16 against the significance level of 5%. This difference highlights the difficulty of arriving at mechanistic models. While correlation is still at about 88.5%, an

improvement to account for 11.5% of correlation is required in order to perfectly predict the real life values.

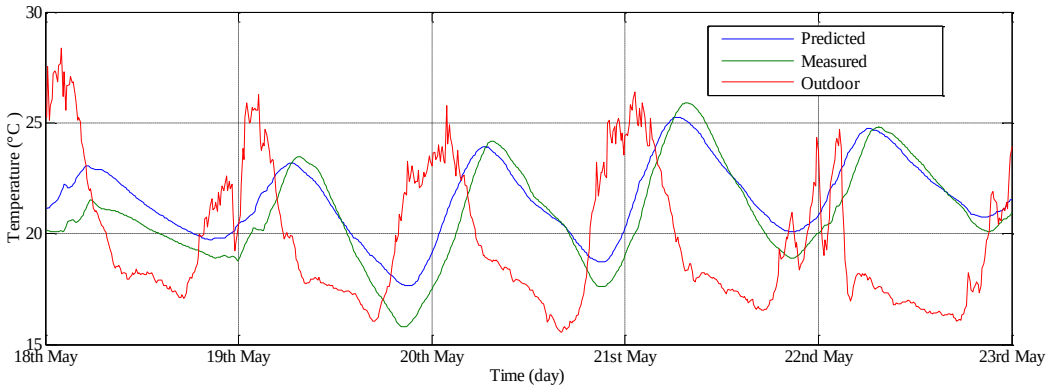

Figure 4.3 Relationship between the measured outdoor temperature, the indoor temperature and the predicted temperature.

4.3 Energy Savings from Green Roof

The most important aspect of green roofs is the energy savings they offer. From a thermal point of view, the effect of green roofed urban buildings on energy cooling loads at no-ventilation were investigated in this study. Heat gain, as a convention was taken to be positive, means cooling has to occur to bring the temperature down to a conducive 23°C. Heat gain for GRUB during daytime, i.e. between 9.00 am and 4.00 pm, for the period of 18th May, 2014 to 6th July, 2014 were compared with that of BRUB. Based on this result, heat gain for BRUB was the ideal case requiring cooling, and the differences recorded for GRUB were compared to determine the percentage in reduction. The result, given as daytime average is shown in Figure 4.4.

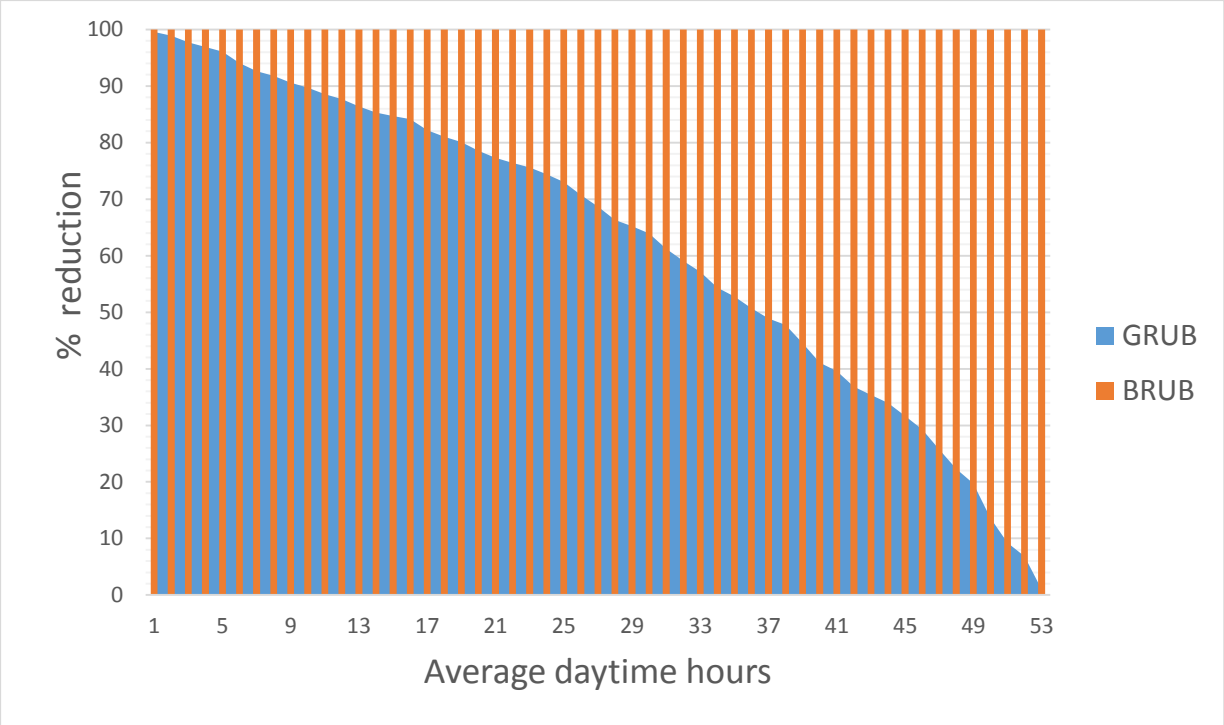

Figure 4.4 Cooling load reduction of GRUB compared with BRUB

The blue bars represents the cooling load reduction of GRUB compared against a 100% case of BRUB, showed in red bars. Results show an average of 62.9% possible cooling load reduction exists during cooling times. This reduction was due to the reduced solar radiation into the building offered by the living green roof. The result means that if for 100% of the time, a bare roofed house needs cooling, a green roof will not require cooling for 63% of that time.

4.4 Differences between Indoor Microclimates of GRUB and BRUB

The results shown in the figures are when House A was covered with the green roof and House B had a bare roof. This treatment will hereafter be referred to as Test A. Values obtained when the green roof was interchanged for the two buildings is hereafter referred

to as Test B. Results from both tests were discussed together. Results from Test A are shown on the figures, while results from Test B are recorded in Tables 4.1 and 4.2.

4.4.1 Temperature

Figure 4.4 shows the graph of temperature recorded by the sensors placed just below the roofs for Test A as shown in Figure 3.3. A maximum and minimum reading of 32.57°C and 17.93°C was recorded in BRUB against 30.51°C and 17.53°C recorded in GRUB. The mean value recorded in the GRUB is 22.86°C while that of BRUB is 24.48°C. The measurements of the green roofed urban building (GRUB) were averagely 1.6°C lower than those recorded in the bare roofed urban building (BRUB). Looking at Figure 4.5, the maximum temperature difference between GRUB and BRUB was recorded as 8.12°C. This huge difference in indoor temperature readings of GRUB and BRUB shows a large potential for reducing the amount of time air conditioners need to be on for cooling the inner environment. Less operating time to bring temperatures down to normal room temperature of 25°C means less energy consumption otherwise called cooling loads.

The investigation of the degree of temperature reduction offered by the green roof showed that an average of 2.16°C difference was maintained during the daytime. See Figure 4.6 for the graphical representation. The peak difference recorded during the daytime was 6.49°C at 2.00pm on 1st June, 2014. In the United States, 1° C increase in temperature would increase peak electricity demand by 2-4% when temperature exceeded 15-20° C (Akbari et al., 1992). This shows that the 2.16 °C difference has a huge significance on the energy consumption. Temperature readings shown on the graph also show peak

temperature delays. During the nights of the observation period, there was an average difference of 3.92°C between the indoor temperature of the green roofed urban building and the outdoor temperature. The lowest difference between the two measurements is negative 7.39°C, recorded at around 1.20am on 2nd June, 2014. This phenomenon shows that green roofs effectively provides thermal insulation during cold weather. Furthermore, this thermal insulation would mean the energy used in heating the indoor environment will be reduced due to heat entrapment. Considering there is no ventilation system, the indoor thermal environment was less fluctuant thus, more heat was conserved.

For Test B, a maximum reading of 28.99 °C was recorded just below the bare roof against 25.82°C recorded in GRUB. Averagely, the indoor temperature in GRUB is 20.91°C and 21.26°C in BRUB. From this, it is quite clear that temperature readings for Test B are all lower than the Test A scenario. A z-test was used to analyse the temperature differences (column 3: B-G, in both tables) recorded between GRUB and BRUB for both Test A and Test B. The results showed that there is a significant difference between the temperature differences of the different treatments. Hence, the difference can be attributed to the closeness of an office block that is just 4m away from GRUB when considering Test B. BRUB for Test B is standing far away from any building, thus favouring airflow in all directions, whereas the office block can be seen to obstruct air flow from the west direction of GRUB.

Table 4.1 Temperature readings (°C) for Test B

	GRUB	BRUB		Outdoor measurement			GRUB	BRUB		Outdoor		
	Sensor below roof		B-G	O	O-G	O-B	Temp btw roof and floor		B-G	Outdoor	O-G	O-B
Mean	20.91	21.26	0.36	18.41	-2.50	-2.85	20.80	20.51	-0.30	18.41	-2.39	-2.10
Standard Error	0.03	0.03	0.02	0.05	0.04	0.02	0.02	0.02	0.01	0.05	0.04	0.03
Standard Deviation	1.71	2.34	1.42	3.26	2.64	1.44	1.62	1.67	0.44	3.26	2.72	2.33
Minimum	16.49	15.46	-2.42	8.42	-8.90	-8.81	16.51	15.63	-1.72	8.42	-8.49	-7.37
Maximum	25.82	28.99	5.56	27.85	4.28	1.24	25.60	25.62	0.94	27.85	4.79	4.32

Key: GRUB = G, BRUB = B, Outdoor = O.

O-G = Temperature/RH difference between outdoor and indoor readings in GRUB.

O-B = Temperature/RH difference between Outdoor and indoor readings in BRUB.

B-G = Temperature/RH difference between GRUB and BRUB values.

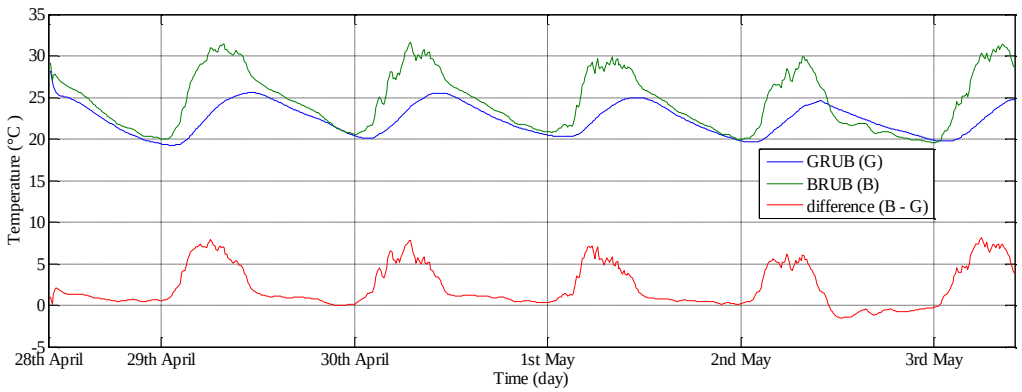

Figure 4.5 Temperature readings just below the green roof

When the outdoor temperature recorded was compared with the previous readings measured inside the buildings for Test A, Figure 4.6, a negative difference was recorded i.e. the temperatures inside the buildings were averagely higher than the temperature outside. This is because of the cold season that crept in during the field study. This is a climate variability. However, during the hottest days, when the outdoor temperature was

higher than the indoor temperatures, the maximum temperature difference recorded was 5.94°C and 0.57°C for GRUB and BRUB respectively. This is the maximum effect the green roofs have shown in heat gain reduction. Thus, less indoor temperature will be recorded if buildings are covered with living vegetation. This is also the same case for Test B but only of lesser magnitude in terms of temperature reduction. The reason for the lower magnitude can be attributed to close proximity of GRUB to an office building as earlier mentioned.

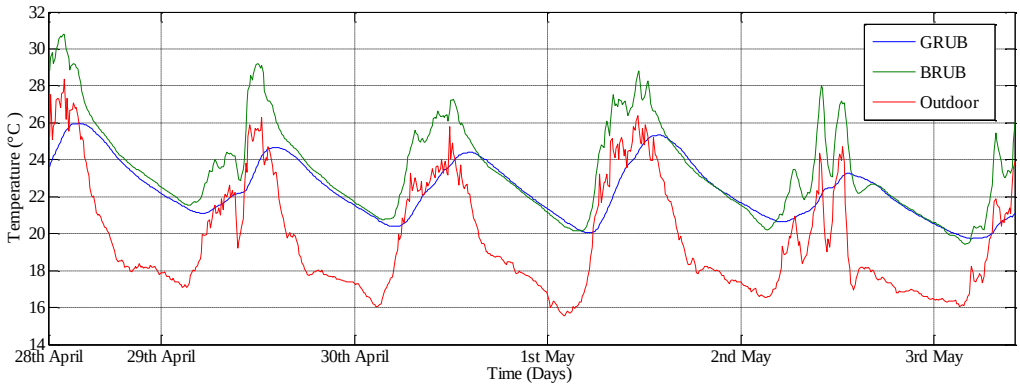

Figure 4.6 Comparison of outdoor and indoor temperature readings obtained just below the roof

Figure 4.7 shows the temperature measured for Test A with the sensor placed just midway position (equidistant from the roof and floor) in the buildings. See Figure 3.3 for the pictorial presentation of sensors in the physical models. An average of 22.5°C and 23.13°C was measured in GRUB and BRUB respectively. Both averages had a standard error of 0.04. There was a maximum temperature difference of 1.67°C between GRUB and BRUB that was recorded. The average mean temperature difference between BRUB

and GRUB was 0.63°C. Compared to the previous average of 1.6°C recorded for temperature readings just below the roofs, this shows a drop in the magnitude. This is due to the invariable nature of heat seeking lower potential always. Despite the fact that the degree in mean temperature differences between the two houses reduced by 0.97, the effect of the green roof in temperature reduction is obvious. This was also the case for Test B. All findings showed similarity to the Test A case. And this was affirmed by a z-test that was carried out to investigate whether there is a significant difference between the means of differences of temperature measurement of Test A and B. The result showed that there is a significant difference between the two measurements.

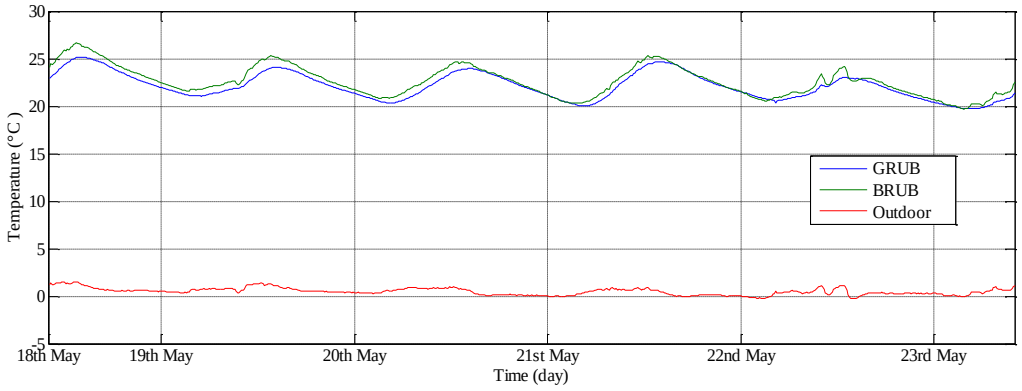

Figure 4.7 Temperature readings measured equidistant between the roof and floor in the two buildings

Figure 4.8 shows the comparison of outdoor temperature measurements with temperature measurements at a halfway between the roof and floor of the in the buildings for Test A. Like with the case of temperature readings just below the roofs, outdoor temperatures here are averagely lower than those measured in the buildings. Same reason of cold

season applies here. An average of -2.20 and -2.80°C between outdoor measurement and the measurements in the GRUB and BRUB were recorded respectively. The differences between outdoor and indoor temperature readings of GRUB and BRUB were compared and the results showed a minimum of -8.42°C and -7.37°C and a maximum of 4.79°C and 4.32°C respectively. For the minimum value that occurred when it was very cold outside shows that GRUB retains more heat gain during the daytime than BRUB. Therefore, the average heating time building users will use their room heaters in order to raise the temperature to a more conducive one is reduced, hence, reducing heating load.

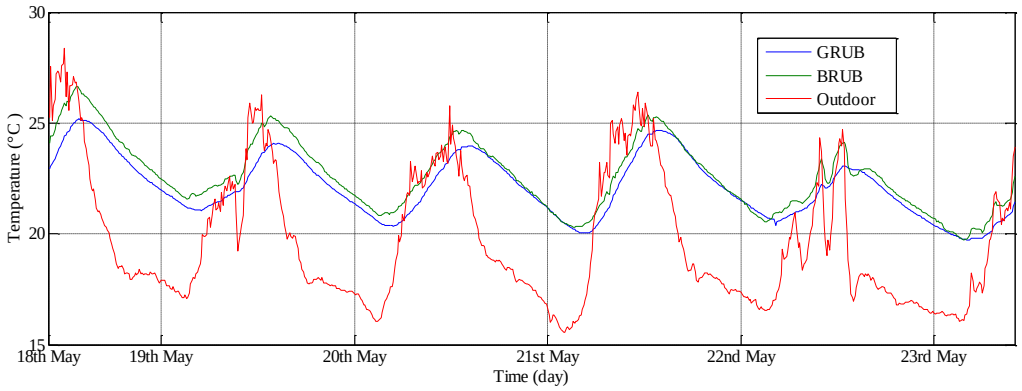

Figure 4.8 Comparison of outdoor temperature with indoor temperature midway in the models

4.4.2 Relative Humidity

Measurements of relative humidity were also carried out at the same points as for the temperature. Figure 4.9 shows the values of relative humidity measured just below the roofs and the differences between BRUB and GRUB values. The mean relative humidity

of GRUB was 91.16% against 75.14% in BRUB. Averagely, the values recorded in GRUB were higher than that recorded in BRUB. An average difference of -16.02% was recorded. The GRUB shows a higher retention capacity for indoor moisture. This is due to the added layer of green roof that not only prevents moisture from getting in, but also from going out. On the 3rd of May, 2014, when the ambient weather was extremely cold, RH readings in both buildings peaked at 100%. This shows moisture escapes faster with the conventional roof when compared with the green roof. Surprisingly, for Test B, the RH didn't tally with the trend of measurements in Test A. BRUB logged higher RH values. An average of 83.63% against GRUB's average of 76.3% was recorded. This awkward result may be possibly due to the high fluctuation rate of the BRUB. Because of less insulation, more RH accrues faster than in GRUB. And considering the measurements obtained in the cold season were long.

Table 4.2 RH readings (%) for Test B

	GRUB	BRUB		Outdoor measurement			GRUB	BRUB		Outdoor		
	RH below roof		B-G	Outdoor	O-G	O-B	RH btw roof and floor		B-G	Outdoor	O-G	O-B
Mean	76.30	83.63	7.33	77.62	0.93	-5.89	76.69	83.51	6.82	77.62	0.93	-5.89
Standard Error	0.08	0.10	0.06	0.21	0.20	0.20	0.07	0.05	0.03	0.21	0.20	0.20
Standard Deviation	5.39	7.09	4.38	14.58	13.74	13.32	4.64	12.94	3.00	14.58	13.74	13.32
Minimum	61.35	59.56	-8.38	39.30	-35.20	-42.20	65.80	70.30	-0.20	39.30	-35.20	-42.20
Maximum	87.65	100.00	19.06	99.70	27.80	17.40	86.10	91.50	12.30	99.70	27.80	17.40

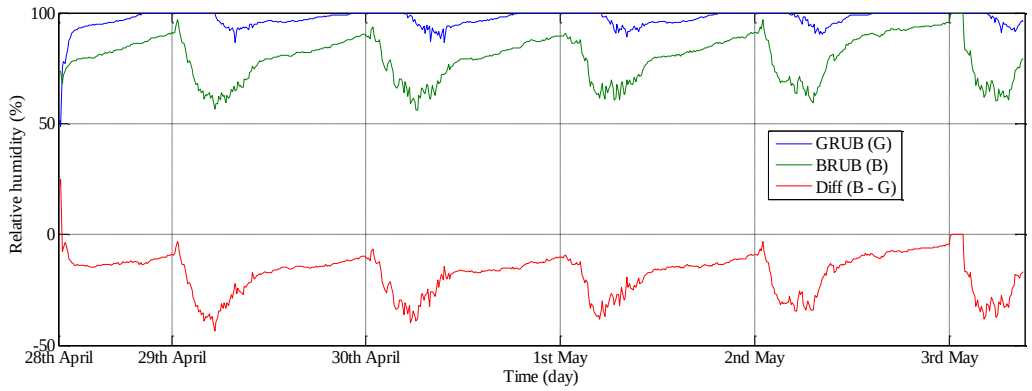

Figure 4.9 Comparison of RH measured just below the roofs.

The outdoor relative humidity measured was compared with the indoor relative humidity measured just below the roofs in both GRUB and BRUB. See Figure 4.10 for the relationship. Outdoor measurements were averagely lower than indoor measurements. When the outdoor measurement was compared with that in GRUB, an average difference of 14.54% was recorded. However, for the BRUB, a small average difference of 0.69% was recorded. The maximum difference between the outdoor RH and GRUB indoor RH is higher than the corresponding value of BRUB.

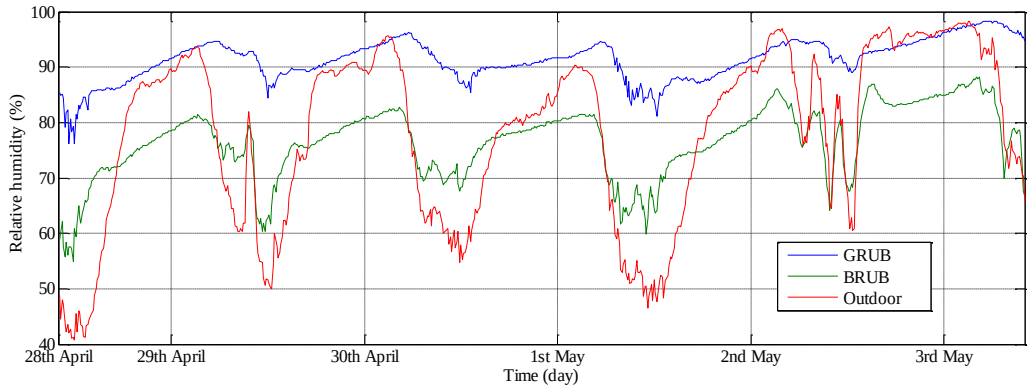

Figure 4.10 Comparison of outdoor and indoor RH measured just below the roof

Figure 4.11 shows values of RH measured midway in both models and their differences. An average of 84.37% was recorded in GRUB against a lower value of 74.8% in BRUB. Both of these averages, when compared with those measured just below the roofs were lower. However, the average minimum values measured midway in the two models are higher than the corresponding values just below the roof. This suggests that the proximity to the roof has a higher potential for changes. Due to the windows being shut, which are mostly at the midway positions of houses, there was no support for quicker fluctuations. Conversely, for Test B, the RH in BRUB are higher than in GRUB. This behaviour suggests the role air flow outside the building plays in cooling off buildings. The GRUB which experiences lower wind effect on its envelope possesses lower RH compared with the values of Test A.

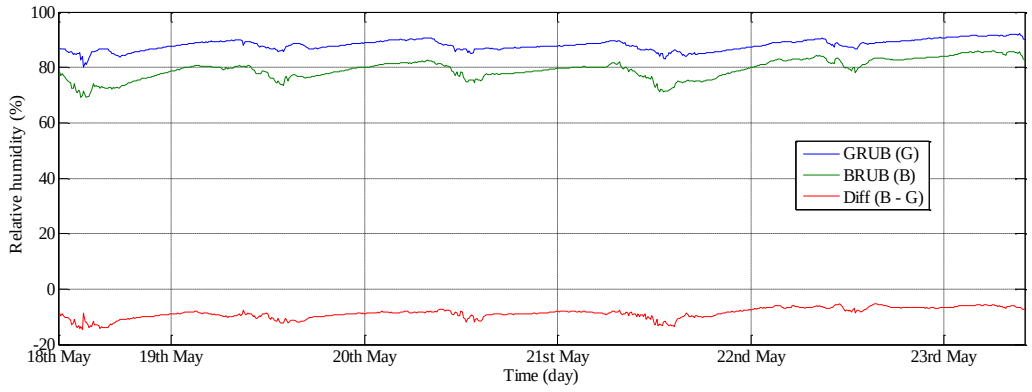

Figure 4.11 Relationship of RH measured in GRUB and BRUB

Figure 4.12 shows the comparison of outdoor RH and indoor RH measured midway in the 2 models. Outdoor measurement was averagely lower than all the indoor readings. At

maximum outdoor RH (98.3%), maximum indoor RH was 92.10% in GRUB and 86.0% in BRUB. At a minimum outdoor RH of 27.10%, indoor measurements were 70.3% in GRUB and 58.1% in BRUB, suggesting more moisture entrapment capacity by GRUB. However this wasn't the trend for Test B. RH values were lower in GRUB as compared to BRUB. This suggests that the higher exposure capacity of BRUB to the environment as opposed to the obstructed office block near the GRUB, enhanced moisture gain and loss in it.

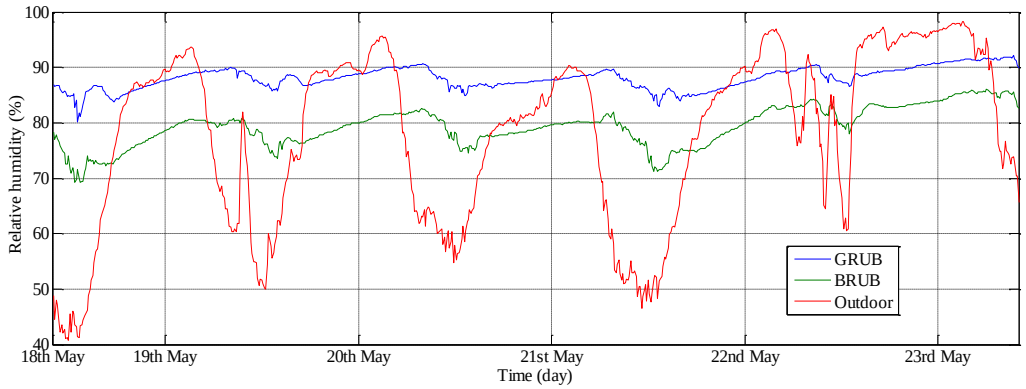

Figure 4.12 Comparison of RH of GRUB, BRUB and with outdoor measurement.

CHAPTER FIVE

CONCLUSIONS AND RECOMMENDATIONS

5.1 CONLCUSIONS

The effect of living green roofs on urban buildings at no-ventilation on cooling loads was investigated in this study. Field scale models, representing urban buildings and singled zoned, were built in Jomo Kenyatta University of Agriculture and Technology campus in Kenya; a green roofed urban building (GRUB) and a bare roofed urban building (BRUB). One was covered with a green roof and the other was left bare. After a month of observation, the green roof was moved to the other model, in order to make reasonable conclusions and remove any bias in errors of measurement.

1. A new computer model, called GRUBCLIM, was developed to predict the indoor air temperature of green roofed urban buildings. GRUBCLIM uses an average U-value as the building specification and the temperature difference between the indoor environment of the house and the ambient outdoor environment. The model was validated and simulated with microclimatic data obtained at the field scale model site. A correlation of 0.885 between the predicted and measured values was recorded.
2. The effect of green roof on cooling energy loads was then investigated. Two models for predicting the cooling load requirement for both GRUB and BRUB were formulated. A comfortable temperature of 23°C was used as a threshold. Any value above it signifies cooling load requirement and any value below it

signifies heating load requirement. Using those two models, an average 62.87% daytime cooling load reduction potential was found to exist. This remarkable potential signifies the beneficial roles living green roofs can offer in terms of energy savings.

3. Indoor microclimate, air temperature and relative humidity parameters, of GRUB and BRUB at no-ventilation were compared. An average of 22.5°C and 23.13°C was measured in GRUB and BRUB respectively. Both averages had a standard error of 0.04. There was a maximum temperature difference of 1.67°C between GRUB and BRUB. The average mean temperature difference between BRUB and GRUB was 0.63°C. The lower temperature value existing in GRUB signifies the effect of the green roof in heat insulation which subsequently reduces the cooling load requirement in GRUB. When differences in temperature readings between Outdoor and indoor temperature of GRUB and BRUB were compared, the results were a minimum of -8.42°C and -7.37°C and a maximum of 4.79°C and 4.32°C respectively. For the minimum value, that occurred when it was very cold outside shows that GRUB retain more heat gained during the daytime than BRUB. An average of 84.37% relative humidity was recorded in GRUB against a lower value of 74.8% in BRUB. Outdoor measurement was averagely lower than all the indoor readings. At maximum outdoor RH (98.3%), maximum indoor RH was 92.10% in GRUB and 86.0% in BRUB. At a minimum outdoor RH of 27.10%, indoor measurements were 70.3% in GRUB and 58.1% in BRUB, suggesting more moisture entrapment capacity by GRUB. The effect of living green roof on the

indoor microclimate of urban building was investigated. Outdoor temperature values obtained around field scale model site were compared with indoor temperature values obtained inside the buildings. On hot days, temperature readings inside the building were always lower than outdoor temperature values. A maximum temperature difference of 5.94°C was recorded at a maximum outdoor temperature was 30.52°C.

5.2 RECOMMENDATIONS

After 2 months of observing two field models, one with a living green roof and the other left bare, research findings and conclusions were reached on the effect of roof greening on urban buildings. Based on those findings, it is safe to recommend the use of living green roofs as elaborated below.

1. The use of living green roofs has shown remarkable reduction of solar radiation that enters buildings. Similarly, green roofed houses offer cooler temperatures when compared to bare roofed houses. A revelation that shows a 1°C temperature difference has a huge impact on energy consumption; an increase of peak electricity by 2-4%. This reduction in temperature consequentially led to the reduction of the times required for cooling to occur. A reduction of cooling times means less operating time for air conditioning equipment and subsequently leading to lower energy consumption. Therefore, with this potential, building owners and developers can start using green roofs in an effort to reduce electricity bills.

2. The new model developed, GRUBCLIM, can be used to predict indoor air temperatures of single zoned urban buildings with a living green roof. The model can help building designers have a working value of what temperature readings houses they are designing could be. This knowledge will help them to better suggest heating, ventilation and air conditioning equipment to use in the house. It will also guide them in designing sizes of windows and doors for natural ventilation.
3. When this study started, average temperature within the region was relatively high. However, as the measurement period extended into July, cold season crept in, and the average temperature became a lot lower than the previous temperatures. This led to shorter measurement period of the effect of green roofs on heat gain reductions in buildings. Future research could consider carrying out his research between the months of January and March, or when the temperature of the area is hottest for a longer period of time.
4. This research could either be conducted in two other scenarios. One is a denser environment with observation models close to other buildings, in order to replicate real life scenarios of urban built environment. And two, is to build the models far away from any obstruction, in order to ascertain the effect of green roofs alone on the heat gain reduction.
5. The new GRUBCLIM could be improved for better identification of parameters and reaching of conclusions. GRUBCLIM only considers the U-value of the building envelope. Future developments could incorporate the heat storage

capacity of each building envelope element. It could also incorporate features such as human activities and effects and heat gain/loss due to ventilation.

REFERENCES

Adrian, C. Z., Hien, W. N., Marcel, I., & Kardinal, J. S. (2013). Predicting the envelope performance of commercial office buildings in Singapore. *Energy and Buildings, 66*, 66-76.

Ajwang, P. (2005). Prediction of the Effects of Insect-Proof Screens on the Climate in Naturally Ventilated Greenhouses in the Humid Tropics.PhD thesis, University of Hamburg, Hannover.

Akbari, H., Davis, S., Dorsano, S., Huang, J., Winert, S. (1992). Cooling Our Communities – A Guidebook on Tree Planting and Light Colored Surfacing. US Environmental Protection Agency, Office of Policy Analysis, Climate Change Division, January.

Akbari, H. (2002). Shade trees reduce building energy use and CO2 emissions from power plants. *Environmental Polltuion, 116*, S119-S126.

Alexandri, E. and Jones, P. (2006). Temperature decrease in an urban canopy due to green walls and roofs in diverse climates. Journal of Building and Environment 43, 480-493.

Barre, H. J., Sammet, L. L. and Nelson, G. L. (1988). Environmental and Functional Engineering of Agricutural Buildings. New York, United States of America: Van Nostrand Reinhold Company Inc.

Barrio, E. P. (1998). Analysis of the green roofs cooling potential in buildings. *Energy and Buildings, 27*, 179-193.

Becker, M. (1986). Heat Transfer: a modern approach. New York: Plenum.

Benevolo, L. (1980). The history of the city. London: Scholar Press.

Castleton, H., Stovin, V., Beck, S. B., & Davison, J. B. (2010). Green roofs; building energy savings and the potential for retrofit. *Energy and Buildings*, 1582-1591.

Chen, R., Kang, E., Ji, X., Yang, J., Wang, J. (2007). An hourly solar radiation model under actual weather and terrain conditions: a case study in Heihe river basin. Energy, issue 32, pp 1148–1157.

Chen, C.-F. (2013). Performance Evaluation and Development Starategies for Green Roofs in Taiwan: A review. *Ecological Engineering, 52*, 51-58.

Cheng, V., Ng, E. and Givoni, B. (2005). Effect of envelope colour and thermal mass on indoor temperatures in hot humid climate. Solar Energy 78, pp. 28-534.

Defraeye, T., Blocken, B., Carmeliet, J. (2010). Convective heat transfer coefficients for exterior building surfaces: Existing correlations and CFD modelling. Energy Conversion and Management.

Drysdale, J. (1976). "Technical Study No. 27," Comm. Exp. Bldg. Station, Australia. Cited by Ogoli, 2003, p. 853

Eastop, T. D. and MConkey, A. (1986). Applied Thermodynamics for Engineering Technologists. 4th ed. Singapore: Longman.

Elias-Ozkan, S. T., Summers, F., Surmeli, N., & Yannas, a. S. (2006). A comparative study of the thermal properties of building materials. *Passive and Low Energy Architecture*, *23*. Geneva.

Gazorli, K. V. (1985). A simple greenhouse climate model. Acta Horticulturae 174, 393-400.

Georgi, J. N. and Dimitriou, D. (2010). The contribution of urban green spaces to the improvement of environment in cities: Case study of Chania, Greece. Journal of Building and Environment. Issue 45, pp 1401-1414.

Givoni, B. (1998). Effectiveness of mass and night ventilation in lowering the indoor daytime temperatures. Energy and Buildings. 28, pp. 25-32.

Graf, A. B. (1992). Colorcyclopedia of exotic plants and trees for warm region horticulture- in cool climates or sheltered indoors. 4th edition. Roehrs Company Publishers, USA.

Granet, I. (1985). Thermodynamics and Heat Power. 3rd Ed. Virginia: Reston.

Huang, H. L. C. Zaheri, M. M. and Hu, E. (2012). "A new zone temperature predictive modeling for energy saving in buildings." Procedia Engineering, 49, pp. 142-151.

Hakansson, A., Hojer, M., Howlet, R. J., Jain, L. C. (2012). Proceedings of the 4th international conference on sustainability in energy and buildings (SEB' 12).

Hui, S. C. M. (2007). Sustainable building technologies for hot and humid climates. Invited paper for the Joint Hong Kong and Hangzhou Seminar for Sustainable Building, 21-23. September, Hangzhou, China.

Humphreys, M.A. and Nicol, J.F. (2012).Outdoor temperature and indoor thermal comfort –raising the precision of the relationships for the 1998 ASHRAE database of field. ASHRAE Transactions 2000, 206 (2), pp. 485-492. Cited by Madhumathi and Sundarraja, 2012.

Jim, C.I. and He, H. (2011). Estimating heat flux transmission of vertical greenery system. Journal of Ecological Engineering, Volume 37, pages 1112-1122.

Jones, W. P. (1985). *Air Conditioning Engineering* (3 ed.). London, Great Britain: Edward Arnold.

Kenya. (2013). Falling Rain Genomics. Internet. http://www.fallingrain.com/world/KE/01/Juja.html [accessed on 12th December, 2013].

Landsberg, H.E. (1981). The Urban Climate. Academic Press, New York.

Larsen, T. S. (2006). *Natural Ventilation Driven by Wind.*Department of Civil Engineering. PhD Thesis, Aalborg University, Denmark.

Long, C. and Sayma, N. (2009). Heat Transfer.Ventus Aps Publishing.

Lui, K. and Minor, J. (2005). Performance evaluation of an extensive green roof, in: Greening Rooftops for Sustainable Communities, Washington, DC.

Ljung, L. (2001). Black-box models from input-output measurements. 18th IEEE Instrumentation and Measurement Technology Conference, Budapest.

Mac Cracken, M. C. (2009). Beyond mitigation potential options for counter-balancing the climatic and environmental consequences of the rising concentrations of greenhouse gases, The World Bank Development Economics, Office of the Senior Vice President and Chief Economist as cited in Santamouris, 2012.

Mathumathi, A. C. & Sundharraja. B. M. (2012). Experimental study of passive cooling of building facade using phase change materials to increase thermal comfort inbuildings in hot humid areas. *International Journal of Energy and Environment, 3*(5), 739-748.

Math Works 1999. Matlab User's Guide. The Math Works Inc., South Natick, MA 01760, USA.

Martin, P. L., & Oughton, D. R. (1995). *Heating & Air Conditoning of Buildings* (8 ed.). Oxford, Great Britain: Butterworth-Heinemann.

Moran, M. J. and Shapiro, H. N. (1995). Fundamentals of Engineering Thermodynamics. 3rd ed. New York: John Wiley & Sons, Inc.

Mills, G. (1997). The radiative effects of buildings groups on single structures. *Energy and Buildings, 25*, 51-61.

National Meteorological Library and Archive website:

http://www.metoffice.gov.uk/media/pdf/n/9/Fact_sheet_No._14.pdf

[accessed on 25 sept 2013].

Nayak, J. K. and Prajapati, J. A. (2006). Thermal performance of buildings in Handbook on Energy Conscious Buildings. Bombay. India Institute of Technology and Solar Energy Centre.

Ng, E., Chen, L., Wang, Y., Yuan, C.(2012). A study on the cooling effects of greening in a high-density city: An experience from Hong Kong. Building and Environment Issue 47, page 256-271.

Ogoli, D. M. (2003). Predicting indoor temperatures in closed buildings with high thermal mass. Energy and Buildings, 35, pp 851-862.

Oke, T. R. (1976). The distinction between canopy and boundary-layer urban heat island. Atmosphere. Issue 14, pp 268-77.

Oke, T.R., Johnson, G.T., Steyn, D.G., Watson, I.D. (1991). Simulation of surface urban heat islands under ‘‘ideal‘‘ conditions at night – Part 2: Diagnosis and causation. Boundary Layer Meteorology. Issue 56, pp 339– 358.

Oliveira, S., Andrade, H., Vaz, Teresa. (2011). The cooling effect of green spaces as a contribution to the mitigation of urban heat-A case study of Lisbon. Building and Environment. Issue 46, pages 2186-2194.

Saadatian, O., Sopian, K., Salleh, E., Lim, C. H., Riffat, S., Saadatian, E., TOudeshki, A. and Sulaiman, M. Y. (2013). A review of energy aspects of green roofs. *Renewable and Sustainable Energy Reviews, 23*, 155-168.

Ondimu, S. N., & Murase, H. (2006). Thermal properties of living roof greening material by inverse modelling. *Applied Engineering in Agriculture: Selected Contributions in Engineering for Agriculture and Other Bioresource Industries, 22*(3), 435-441.

Ondimu, S. N., & Murase, H. (2007). Combining Galerkin methods and neural networks analysis to inversely determine thermal conductivity of living green roof materials. *Biosystems Engineering, 96*(4), 541-550.

Parizotto, S. and Lamberts, R. (2011). Investigation of green roof thermal performance in temperate climate: a case study of an experimental buildingin Florianopolis. Energy and Buildings. Vol 43 (7), pp 1712-1722.

Priyadarsini, R., Hien, W. N., David C. K. W. (2008). Microclimatic modeling of the urban thermal environment of Singapore to mitigate urban heat island. Journal of Solar Energy Issue 82, pages 727-745.

Raychaudhury, B. C. and Chaudhury, N. K. D. (1961). Thermal performance of dwelling in the tropics, in Proceedings of the Symposium on the Functional Efficiency of Buildings, CBRI, November, pp. 38–42. Cited by Ogoli, 2003, p. 853.

Sjoberg, J., Zhang, Q., Ljung, L., Benveniste, A., Deylon, B., GLorennec, P., Hjalmarsson, H. and Juditsky, N. (1995). Nonliner black-box modelling in system identification: a unified overview. Automatica, vol 31, 12, sections 1 and 31.

Sailor, D. J. (2008). A green roof model for building energy simulation programs. *Energy and Buildings, 40*, 1466-1478.

Salat, R., Awtonink, M., Korpysz, K. (2013). Black-box system identification by means of support vector regression and imperialist competitive algorithm. Przeglad electrotechniczny. ISSN 0033-2097, R89 9 2013.

Santamouris, M. (2001). Energy and climate in the urban built environment. James and James Science Publishers, London. pp 145-159.

Santamouris, M. (2007). Heat island research in Europe – the State of the art. Journal Advances Building Energy Research. Issue 1, pp 123–150.

Santamouris, M., Synnefa, A. and Karlessi, T. (2011). Using advanced cool materials in the urban built environment to mitigate heat islands and improve thermal comfort conditions. Sol. Energy, 85 (12) (2011), pp. 3085–3102

Santamouris, M., Gaitani, N., Spanou, A., Saliari, M., Giannopoulou, K., Vasilakopoulou, K., Kardomateas, T. (2012). *Using cool paving materials to improve microclimate of urban areas - Design realization and results of the flisvos project. Building and Environment*, 53,128-136.

Santamouris, M. (2012). Cooling the cities – A review of reflective and green roof mitigation technologies to fight heat island and improve comfort in urban environments. Sol.Energy http://dx.doi.org/10.1016/j.solener.2012.07.003

Taha, H. H. Akbari, H., and A. Rosenfeld, A. (1989). Vegetation microclimate measurements:the Davis project, Lawrence Berkeley Lab. Rep. 24593.

Taha, H., Akbari, H., and A. Rosenfeld, A. (1991). Heat island and oasis effects of vegetative canopies: Micrometeorological field measurements, Theory and Applied Climatology. Issue 44. pp 123.

Taha, H. (1997). Urban climates and heat islands: albedo, evapotranspiration, and anthropogenic heat. Energy and Buildings Issue 25, pp 99-103.

Taha, H. Akbari and A. Rosenfeld. (1998). Residential cooling loads and the urban heat island: the effects of albedo, Build. Enwon. Issue 23 pp 271.

Tariku, F. (2008). Whole Building Heat and Moisture Analysis. PhD Thesis. Concordia University, Montreal, Quebec, Canada.

Tham, M. (2000). Overview of Mechanistic Modelling Techniques. Department of Chemical and Processing Engineering Lecture Notes. Newcastle upon Tyne. .

Thurow, C. (1983). Improving street climate through urban design, American Planning Association.

Watkins, R., J. Palmer, M. Kolokotroni, P. Littlefair. (2002). The London Heat Island – results from summertime monitoring, Building Services Engineering Research and Technology 23 (2) 97–106.

United Nations. (2011). Department of Economic and Social Affairs, Population Division: World Urbanization Prospects: The 2011 Revision, New York.

United States Central Intelligence Agency website https://www.cia.gov/library/publications/the-world-factbook/fields/2212.html [accessed on 27th September, 2013].

Zinzi, M. (2010). Cool materials and cool roofs; potentialities in Mediterranean buildings. Advances in Building Energy Research 4 (1), pp. 201-266 as cited in Santamouris, 2012.

APPENDICES

Appendix I: List of Publications

Gulma, S. A., Ajwang, P., Ondimu, S. N. (2014). Thermal modelling of green roofed urban buildings. *International journal of advances in engineering and technology*. Vol. 7, Issue 4, pp. 1179-1190.

Gulma, S. A., Ajwang, P., Ondimu, S. N., Wariara, K. (2014). Field evaluation of indoor microclimates of green and bare roofed urban buildings at no ventilation condition in sub-Saharan Africa. *American Journal of Civil Engineering.*

Appendix II: Part of the data used for the experiment

	Time	1	2	3	4	5	6
S/N		695520	695520	695520	695520	695520	695520
Type		TGU-4500	TGU-4500	TGU-4500	TGU-4500	TGU-4500	TGU-4500
Description		Green roof	Green roof	Green roof	Green roof	Green roof	Green roof
Property		Maximum	Temperatu	Minimum T	Maximum H	Humidity	Minimum Hu
1	09/05/2014 09:04		22.729 °C			71.2 %RH	
2	09/05/2014 09:14	24.003 °C	23.585 °C	22.882 °C	83.0 %RH	83.0 %RH	65.1 %RH
3	09/05/2014 09:24	23.395 °C	22.177 °C	22.177 °C	90.9 %RH	90.9 %RH	83.8 %RH
4	09/05/2014 09:34	22.089 °C	21.502 °C	21.502 °C	95.5 %RH	95.5 %RH	91.2 %RH
5	09/05/2014 09:44	21.446 °C	21.175 °C	21.175 °C	97.7 %RH	97.7 %RH	95.8 %RH
6	09/05/2014 09:54	21.155 °C	21.040 °C	21.040 °C	98.8 %RH	98.8 %RH	97.7 %RH
7	09/05/2014 10:04	21.034 °C	21.025 °C	21.020 °C	99.7 %RH	99.4 %RH	98.2 %RH
8	09/05/2014 10:14	21.037 °C	21.037 °C	21.024 °C	100.0 %RH	100.0 %RH	99.7 %RH
9	09/05/2014 10:24	21.083 °C	21.083 °C	21.034 °C	100.0 %RH	100.0 %RH	99.9 %RH
10	09/05/2014 10:34	21.140 °C	21.140 °C	21.090 °C	100.0 %RH	100.0 %RH	99.4 %RH
11	09/05/2014 10:44	21.211 °C	21.211 °C	21.148 °C	100.0 %RH	100.0 %RH	99.9 %RH
12	09/05/2014 10:54	21.296 °C	21.296 °C	21.220 °C	100.0 %RH	99.4 %RH	99.4 %RH
13	09/05/2014 11:04	21.385 °C	21.385 °C	21.306 °C	100.0 %RH	100.0 %RH	99.7 %RH
14	09/05/2014 11:14	21.485 °C	21.485 °C	21.391 °C	100.0 %RH	99.9 %RH	99.9 %RH
15	09/05/2014 11:24	21.622 °C	21.622 °C	21.502 °C	99.7 %RH	99.4 %RH	99.4 %RH
16	09/05/2014 11:34	21.753 °C	21.753 °C	21.637 °C	99.4 %RH	99.4 %RH	98.5 %RH
17	09/05/2014 11:44	21.862 °C	21.862 °C	21.761 °C	99.9 %RH	99.1 %RH	99.1 %RH
18	09/05/2014 11:54	22.024 °C	22.024 °C	21.882 °C	99.4 %RH	99.1 %RH	98.8 %RH
19	09/05/2014 12:04	22.164 °C	22.164 °C	22.038 °C	99.4 %RH	99.4 %RH	98.5 %RH
20	09/05/2014 12:14	22.302 °C	22.302 °C	22.177 °C	99.4 %RH	98.0 %RH	98.0 %RH
21	09/05/2014 12:24	22.427 °C	22.427 °C	22.313 °C	98.2 %RH	98.0 %RH	97.4 %RH
22	09/05/2014 12:34	22.532 °C	22.532 °C	22.435 °C	98.2 %RH	97.4 %RH	97.4 %RH
23	09/05/2014 12:44	22.645 °C	22.645 °C	22.544 °C	97.7 %RH	97.7 %RH	96.9 %RH
24	09/05/2014 12:54	22.761 °C	22.761 °C	22.656 °C	98.2 %RH	98.0 %RH	97.4 %RH
25	09/05/2014 13:04	22.859 °C	22.859 °C	22.771 °C	98.0 %RH	98.0 %RH	97.2 %RH
26	09/05/2014 13:14	22.944 °C	22.944 °C	22.868 °C	98.5 %RH	98.5 %RH	97.2 %RH
27	09/05/2014 13:24	23.047 °C	23.047 °C	22.956 °C	98.5 %RH	97.4 %RH	97.4 %RH
28	09/05/2014 13:34	23.141 °C	23.141 °C	23.056 °C	97.7 %RH	97.7 %RH	96.9 %RH
29	09/05/2014 13:44	23.246 °C	23.246 °C	23.154 °C	98.2 %RH	96.9 %RH	96.9 %RH
30	09/05/2014 13:54	23.370 °C	23.370 °C	23.246 °C	97.7 %RH	97.4 %RH	97.2 %RH

Date Time	Wind Direction	Wind Speed	Gust Speed	Solar Radiation	Temp, °C	RH, %
5/6/2014 9:00	198	0	1.01	190.6	22.034	80.2
5/6/2014 9:10	178.3	0	0.76	114.4	21.939	80.9
5/6/2014 9:20	110.9	0	1.01	136.9	21.891	81
5/6/2014 9:30	85.6	0	0.5	131.9	21.891	81.1
5/6/2014 9:40	84.2	0	1.01	210.6	21.915	81.2
5/6/2014 9:50	84.2	0	1.26	271.9	21.987	80.9
5/6/2014 10:00	84.2	0	1.51	300.6	22.058	80.8
5/6/2014 10:10	301.8	0	1.01	255.6	22.106	81.5
5/6/2014 10:20	258.3	0.25	1.51	208.1	22.13	81.5
5/6/2014 10:30	327.1	0.76	2.77	248.1	22.13	81.7
5/6/2014 10:40	332.7	1.01	2.52	418.1	22.202	81.4
5/6/2014 10:50	11.2	0.76	3.02	444.4	22.345	81.4
5/6/2014 11:00	351	0.5	2.27	463.1	22.417	81.8
5/6/2014 11:10	5.6	0.76	2.52	644.4	22.561	81.5
5/6/2014 11:20	331.3	0.76	3.78	729.4	22.872	80.8
5/6/2014 11:30	349.6	0.5	2.77	496.9	23.016	80.5
5/6/2014 11:40	43.5	0.5	2.52	275.6	23.016	80.8
5/6/2014 11:50	352.4	0.5	2.77	346.9	22.944	81.4
5/6/2014 12:00	7	0.5	2.27	354.4	23.136	81.1
5/6/2014 12:10	338.3	0.76	2.77	266.9	23.088	81.3
5/6/2014 12:20	327.1	0.5	2.27	924.4	23.232	81.3
5/6/2014 12:30	14	1.01	2.77	380.6	23.448	80.3
5/6/2014 12:40	355.2	0.76	2.52	436.9	23.497	80.8
5/6/2014 12:50	352.4	0.5	2.27	970.6	23.641	80.7
5/6/2014 13:00	355.2	0.76	3.27	394.4	23.833	80.4
5/6/2014 13:10	325.7	0.76	4.28	570.6	23.857	80.7
5/6/2014 13:20	335.5	0.76	3.53	846.9	24.146	80.1
5/6/2014 13:30	320.1	1.01	3.53	1024.4	24.388	79.4
5/6/2014 13:40	345.4	1.01	3.27	415.6	24.581	79
5/6/2014 13:50	321.5	0.76	2.52	365.6	24.557	79.5

Plate 1.0 Bare roofed urban building closer to the office block

Plate 2.0: Green roofed urban building